Faculty of Technology and Science
Chemical Engineering

Erik Bohlin

Optics of coated paperboard

Aspects of surface treatment on porous structures

Karlstad University Studies
2011:1

Erik Bohlin

Optics of coated paperboard

Aspects of surface treatment on porous structures

Karlstad University Studies
2011:1

Erik Bohlin. *Optics of coated paperboard – Aspects of surface treatment on porous structures*

Licentiate thesis

Karlstad University Studies 2011:1
ISSN 1403-8099
ISBN 978-91-7063-333-1

Distribution:
Karlstad Universiy
Faculty of Technology and Science
Chemical Engineering
SE-651 88 Karlstad, Sweden
+46 54 700 10 00

www.kau.se

Print: Universitetstryckeriet, Karlstad 2010

Abstract

Calendering of coated and uncoated paper is widely used to enhance optical properties such as gloss and print quality. The aim of this thesis is to characterize coatings and prints, and to validate models using experimental results from optical measurements of physical samples.

Calendering of coated paper often leads to a brightness decrease. The mechanism for this is not altogether clear. One common explanation is that the porosity of the coating layer decreases and hence that the light scattering power decreases. By comparing simulated and measured results, it was shown that modifications of the surface properties account for the brightness decrease with calendering of substrates coated with ground calcium carbonate. Monte Carlo light scattering simulations, taking into account the measured decrease in surface micro-roughness and the increase of the effective refractive index, showed that surface modifications accounted for most of the observed brightness decrease, whereas the bulk light scattering and light absorption coefficients were not affected by calendering. It was also shown that the scattering coefficient is significantly dependent on the coat weight whereas the physical absorption coefficient is not.

The penetration of ink in the z-direction into a substrate influences the quality of the print. The ink penetration affects the print density, mottling and dot gain, common print effects that influence achievable print quality and visual appearance. The pressure in the printing nip and the porosity of the substrate both affect the amount of ink that is pressed into the porous structure of a coating layer during printing. By printing pilot-coated paperboard with different coating porosities and measuring the resulting optical properties of the prints, a basis for simulations of the different layers, that is to say the coating, the print and the mixed layer in between, was created. Results show that ink distribution is strongly affected by the roughness of the substrate. Fibres and fibre flocks underneath the two coating layers created an unevenly distributed coating thickness that affected the print quality. Differences in pore size and pore size distribution also affected the behaviour of the ink. A coating layer of broad pigment particle size distribution resulted in a relatively low print density, in comparison to coatings of narrowly distributed particle sizes. Comparison of dot gain showed that the coating layer of a narrow particle size distribution had a relatively low dot gain compared to other pigment size distributions used. In this work, these results are explained by the differences in ink distributions on and in the coating layers.

Papers included in this thesis

I. Bohlin, E., Coppel, L., Andersson, C., Edström, P. (2009): *Characterization and Modelling of the Effect of Calendering on Coated Polyester Film.* Advances in Printing and Media Technology, In N. Enlund and M. Lovreček (ed)., Advances in Printing and Media Technology, Vol. XXXVI, Proceedings of the 36th International Research Conference of iarigai, Stockholm, Sweden, September 2009, p. 301-308. Darmstadt, Germany, ISBN 987-3-9812704-1-0.

II. Bohlin, E., Coppel, L., Johansson, C. and Edström, P. (2010): *Modelling of Brightness Decrease in Coated Cartonboard as an Effect of Calendering – Micro-roughness and Effective Refractive Index Aspects.* TAPPI 11th Advanced Coating Fundamentals Symposium, Munich, Germany, October 11-13, 2010. Symposium Proceedings, TAPPI Press, Norcross, GA, USA, ISBN 1-59510-203-5, p. 51-65.

III. Bohlin, E., Johansson, C. and Lestelius, M. (2010): *Flexographic Ink-Coating Interactions, Effects of Porous Structure Variations of Coated Paperboard.* Manuscript in preparation.

Reprints have been made with permission.

Erik Bohlin's contribution to the papers

Erik Bohlin performed all the experimental work with the exception of the Monte-Carlo simulations and the reflectometry measurements in Paper I and Paper II, and the mercury porosity measurements in Paper III. Erik Bohlin is the main author of these three papers.

Table of contents

1 Introduction

1.1 Optical properties

We are all each day confronted with a large amount of more or less important information that we have to consider, and even in our digital society we need paper for communication, documentation and education. Paper in different forms also has a wide range of other uses, as for example packaging materials, paper towels, construction materials and for decorative purposes. Much of the paper we use or are confronted by in our daily life, such as newspapers, books and packages, contains printed images or texts, and the appearance of both the print and the supporting surface is of importance. A good contrast between a printed text and the paper makes it easier to read, a detailed print of an illustration make it more informative, and clear and evenly distributed colours on a package or on a poster makes it more appealing. All of these qualities depend on the optical properties of both the paper and the print, that is to say on the behaviour of light illuminating the different materials.

Coating to improve the appearance and printability of the relatively rough surfaces of a paper is a commonly used method in the papermaking industry, and the technique is often compared to painting, where paint is applied for example to a rough wood surface for very much the same reason. The coating process increases the production cost and it is therefore used mainly when the appearance of the product is of great importance, such as for posters, magazines and illustrated books. However, sometimes other issues are prioritized. In newspapers, the paper is not coated. The main purpose of a newspaper is to deliver information quickly and cheaply and the print quality is of secondary importance, and we can therefore accept lower contrasts and poorer image details. Paper used for newspapers is however often calendered.

Calendering of coated and uncoated paper is widely used to enhance the optical properties such as gloss and print quality. The beating of paper sheets to make the surface smoother is a technique that may be as old as paper itself, and the mechanized technique as we know it today, where two rolls compress the paper web under an adjustable line load and at an appropriate temperature, was introduced in the 1820's. The calendering technique has undergone a constant development since then, and numerous studies have been undertaken to investigate the impact of calendering on the optical properties of the paper.

It is not only the smoothness of the surface that is affected when a paper is calendered. The compression of the substrate changes the structure and the porosity of both paper and coating layer, and this often leads to unwanted changes in the optical properties, such as a loss of opacity and brightness, as well as a decrease in mechanical strength. When the Kubelka-Munk equations are used, the decrease in brightness often found to be associated with a decrease in the light scattering coefficient, an effect that has sometimes been attributed to a homogeneous compression of the coating layer (Pauler 1999; Larsson et al. 2006). However, it has also been suggested that the effect can be explained by a decrease in the micro-roughness of the surface of the coating layer. An important factor to consider when this effect is studied is the temperature in the calender nip. Due to unevenly distributed heat, an increase in temperature at a low line load affects the surface more than the underlying layers, an effect that has been confirmed for both uncoated and coated papers (Rounsley 1991; Park & Lee 2006).

Neither a paper nor a coating layer can be considered to be homogeneous. The shapes, sizes and amounts of different particles create complex structures that can change throughout the thickness direction and, although a coating layer makes a paper more smooth, the thickness varies on a large and a small scale due to the roughness of the substrate. This has been reported to create local variations in density and surface porosity, or so-called closed areas, effects that increase considerably with calendering. The unevenly distributed structure has also been attributed to particle migration in the coating layer during drying. A rapid water evaporation lead to an accumulation of small binder particles in the coating surface layer and thereby create porosity and surface energy differences due to local variations in thickness and density.

The local structural differences on a coating surface have a high impact on printing, and an uneven ink distribution and uneven ink absorption are a common problem when printed products are manufactured. This effect, called mottling, appears as a speckled and uneven print and can be described as unwanted reflectance variations. Although variables in the printing procedure such as speed and line load affect the print quality, mottling is mostly attributed to the properties of the substrate. The coverage of ink on the substrate, or the print density, is also often used as a measure of print quality. The penetration of ink into the coating layer has been shown to greatly affect the print density. A more porous coating structure increases the ink penetration, and as a result, the print density decreases.

1.2 Modeling

For a long time, the well-known Kubelka-Munk equations have been the major model for the simulation of optical properties in the paper industry. Due to their simplicity their use is still widespread even though their limitations are well known and have been discussed in several scientific articles. However, despite the assumptions, such as for example a flat surface, a homogeneous layer and a two-flux system, the Kubelka-Munk model is often sufficient when certain optical properties are investigated. In other cases, when information regarding refractive index, multi-flux or surface structures is treated, alternative methods are needed. More recently, theories based on radiative transfer theory have been developed to calculate the optical response given almost any illumination and detection geometry. These theories also handle heavily dyed papers, full-tone prints, gloss and the effects of optical brightening agents.

The PaperOpt project aims at modelling the paper optical system as a whole, including the optical influence of all paper components and surface treatments, from printing methods and inks to measurement and evaluation, in order to facilitate efficient product development and production methods for papermaking and printing, as well as improving printing quality and colour reproduction for a lower ink consumption. The Open PaperOpt model is a simulation program that has been designed to calculate of light scattering and light absorption in paper and paper coatings (Coppel & Edström 2009). It uses a probability approach that takes into account structures both inside the layer and on the surface of the simulated sample. One of the major goals of the PaperOpt project is to suggest principles for achieving a more correct interpretation of reflectance factor measurements in order to facilitate efficient and correct data exchange between the paper and printing industries. Another goal is to develop simulation tools for the prediction of optical properties and print quality from paper properties and process parameters.

1.3 Objective and content

The aim of the work described in this thesis is to characterize coatings and prints, and to test models against experimental results from optical measurements on physical samples. It summarizes the results published in three papers. The first two papers cover the brightness decrease of calendered coating layers of different composition, applied on both absorbent and non-absorbent substrates, and the third paper focuses on ink penetration and the resulting variations in print mottle and print density on printed coating layers of different porosities.

The purpose of Paper I was to simulate the decrease in brightness of coating layers after calendering. Results from optical measurements of laboratory-coated samples were compared to simulated values. In order to eliminate the effect of the substrate and to determine the optical properties of the coating colour alone, a non-absorbing plastic film was used as substrate. A decrease in brightness was detected in all the samples, and results from the simulations indicated that this could be attributed to a decrease in surface micro-roughness and a decrease in the effective refractive index. This result was supported by the finding that the thickness of the coated substrate was unaffected by the calendering.

In Paper II, the investigations were extended to a coated paper substrate. Plastic films were also coated for comparative purposes. It was shown that the brightness decrease of the cartonboard substrate due to calendering had a negligible contribution to the total brightness decrease of the coated cartonboard. Although the brightness decrease was lower for the coated cartonboard than for the non-absorbing substrate studied in Paper I, the decrease in this case could also be attributed to a decrease in the surface micro-roughness and a decrease in the effective refractive index.

In the interphase between a coating layer and a layer of applied ink, coating material and ink will be mixed. The depth of this mixed ink/coating layer region depends on the porosity of the coating layer and on the amount of ink penetration. The amount of water-based flexographic ink penetrated into coating layers of three different porosities and its effect on print quality was studied in Paper III. A coating layer containing a pigment with a broad particle size distribution showed the lowest print density, while coating layers containing either pigments of narrow particle size distribution or pigments of small particle size showed equal and higher print density values. Print density increased and dot gain decreased as the coating pore structure became more open. The results indicate that a relatively large pore diameter and a large pore volume was beneficial for print quality with a water-based flexographic ink.

2 Coating for improved optical properties

To achieve a smoother and a more printable surface, paper and paperboard grades are often coated. The coating layer is applied to the substrate as a wet coating colour by several coating techniques, which will be discussed later in this thesis. The coating colour consists of pigments, binder, thickener and water. Additives are also sometimes used to improve certain properties. The solids content of a coating colour can vary between 50 and 70 % depending on the properties of the substrate, the required rheological properties of the coating colour, the coating technique, the coating speed and other parameters. In industrial coating, it is desirable to keep the solids content as high as possible, partly for environmental reasons, partly to save energy in the drying stage which has a large impact on the process economics. Under laboratory conditions, however, where the coating speed is considerably lower and unconventional substrates are sometimes used, a coating colour of low solids content is often more favorable.

The substrate can be coated in a single layer or in several layers as, shown in Figure 1. A common technique is to apply a pre-coating to cover the fibre surface and to provide a smooth base for the subsequent application of one or two top-coatings to improve the optical properties and printability. A dry coating layer has a typical coat weight of 5-20 g/m^2 with a thickness of 5-20 μm.

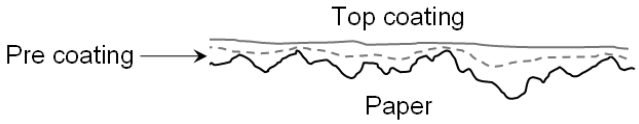

Figure 1. A paper with two coating layers. The pre coating levels out the rough surface of the paper while the top coating creates a smooth surface.

2.1 Pigments

The major constituent of a coating colour is the pigment. Calcium carbonate, kaolin clay, talc or a mix of these are the most commonly used pigments. Calcium carbonate, either ground (GCC) or precipitated (PCC), is a very white mineral consisting of nearly sphere-shaped particles. Kaolin clay on the other hand consists of disc-shaped particles having a slightly lower whiteness. For this reason, calcium carbonate is often used when a white surface is prioritized, while kaolin clay is used to obtain a good coverage and a smooth and glossy surface. However, the use of a fine-particle calcium carbonate grade can result in gloss values above those obtained with certain kaolin clays. Commercial coating pigments are available in a

wide range of particle sizes, particle shapes and particle size distributions (PSD). By mixing different pigments, coating layers with broad variations in porosity, structure and surface properties can be created.

Clay particles have negatively charged surfaces and positively charged edges (Figure 2) and clay particles tend therefore to attract each other and form aggregates, so called house-of-cards structures. The adsorption of a dispersing agent added under alkaline conditions renders the edges more negatively charged, and the dispersion stability can thus be increased. However, alignment of the plate-like particles in a loose house-of-cards structure yields an open and porous dry coating layer. Compared to the more close-packed structure formed by spherical GCC pigments, clay particles are more able to reorient themselves and clay coatings are thus considered to be more compressible (Larsson et al. 2006; Dean 1997).

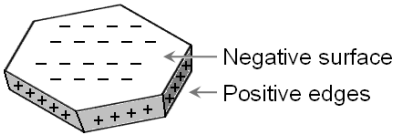

Figure 2. The electrical charges on a clay particle.

The optical properties of a coating layer are strongly influenced by the particle size and PSD of the pigment, properties that affect the particle packing and the surface structure. It is convenient to describe the pigment particle size using a single number that represents the weight percentage of particles below a specified size. A cumulative size distribution curve, as shown in Figure 3, provides information about the PSD. The weight percentage on the y axis is plotted against the measured particle size on the x axis. The weight percentage gives information about the quantity of particles that are smaller than a given particle size (Dean 1997).

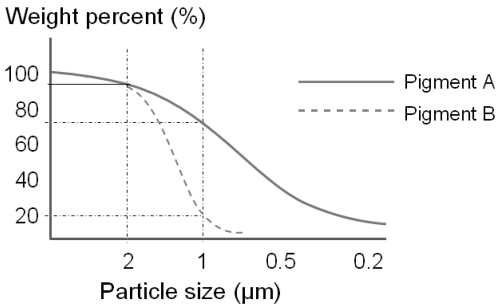

Figure 3. Example of a cumulative size distribution curve. Measurements of particle size of two pigments are shown, pigment A represented by a dashed line and pigment B by a solid line. About 90% of the particles of both pigments are less than 2 µm in size, but pigment A has a less steep slope, and thus a broader particle size distribution.

Figure 3 shows data from particle size measurements by a sedimentation technique (Sedigraph) for two different pigments. About 90% of the particles are less than 2 µm in size for both pigment grades, but pigment A has a broader particle size distribution. The proportions of particles below 1 µm in size is about 70% for pigment A and about 20% for pigment B, which shows that pigment A contains a larger number of "small" particles and thus has a broader PSD.

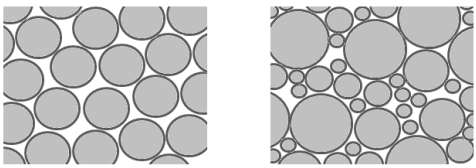

Figure 4. Illustrations of a narrow (left) and a broad (right) PSD. The small particles in a pigment of broad PSD occupy the space between the larger particles, and this results in a more close-packed structure.

A narrow PSD leads to a more open (porous) structure caused by the packing of the particles (Figure 4) (Lepoutre & De Grace 1978). It has been found that a PCC coating with a narrow PSD gave enhanced optical properties (Preston et al. 2008). The narrow PSD gave higher gloss and higher brightness, and measurements showed that this coating also had a low micro-roughness. It has also been found that the addition of clay to a PCC slurry reduced the porosity due to a denser packing of the particles(Larsson et al. 2006; Preston et al. 2008).

2.2 Binders

Latex is used in coating colour formulations to bind the pigment particles to each other and to the substrate. Latices are composed mainly of polymer particles dispersed in water, commonly consisting of styrene-butadiene (SB) or styrene-acrylate (SA) copolymers, and film formation initially takes place as a result of water evaporation. Several theories have been proposed to explain the film formation, but it is classically said to take place in a stepwise manner (Figure 5) (Dobler & Holl 1996). After the evaporation of the water, the particles are ordered and closely packed. The particles then undergo deformation due to capillary forces. In the final step the particle structure collapses due to an inter-diffusion of polymer chains over the particle boundaries. The temperature at which film formation occurs is closely related to the glass transition temperature (T_g) of the co-polymer. The T_g is thus an important property of the latex, and it can be designed to fit specific coating property requirements.

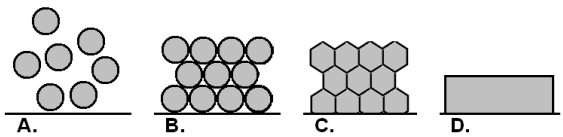

Figure 5. A: latex particles dispersed in water, B: evaporation of water and the formation of a packed structure, C: deformation of particles and C: film formation.

Analyses have shown that a higher latex content in the coating layer leads to a greater compression during calendering (Larsson et al. 2006).This study also showed that the gloss decreased with increasing latex content due to the increase in surface roughness as determined by atomic force microscopy. After calendering, however, the gloss values were roughly the same for samples containing different amounts of latex.

Other studies have also confirmed the greater gloss variation when more latex is added to the coating colour. In one study (Preston et al. 2008), several pigments of different sizes and different PSDs were combined with latex at addition levels of 9, 12, 15 and 18 parts per hundred parts of pigment. Both gloss and brightness clearly decreased with increasing amount of latex, and reflectometry measurements also showed that the micro-roughness increased with increasing binder addition.

The particle size of the latex has been shown to affect the porosity of the coating layer. In a study in which coatings containing different lattices were compared, the

coating colour containing the latex with the smallest particle size showed the greatest number of pores per surface area and also the smallest pore size (Lamminmaki et al. 2005). The larger the latex particle size, the fewer were the number of pores per unit area and the larger was the pore diameter.

To reach satisfactory and smooth coating properties, it is desirable to have a uniform distribution of latex through the coating layer. However, small latex particles move during the coating film formation and behave differently from the relatively much larger pigment particles (Kenttä & Pohler 2008). The extent to which latex migration occurs within the coating layer depends both on the properties of the latex particles themselves, and on other factors in the system such as the type of co-binder, the drying conditions and the amount of water absorbed into the paper substrate.

Latex migration occurs when the coating layer has reached the immobilization stage, where the relatively large pigment particles have formed a structure (Zang et al. 2008). The remaining water either evaporates at the coating-air interface or moves upwards through the coating layer due to capillary forces, or is absorbed into the base paper (Figure 6). The latex particles, which are much smaller than the pigment particles, follow the water through the pore structure, and can thus accumulate either at the top or at the bottom of the coating layer. In other words, latex migration is strongly related to the water retention ability of the coating. Other factors are the ability of the substrate to absorb water, the drying temperature and the speed of the drying process, the type of coating applicator and the composition of the coating colour (Aschan 1973).

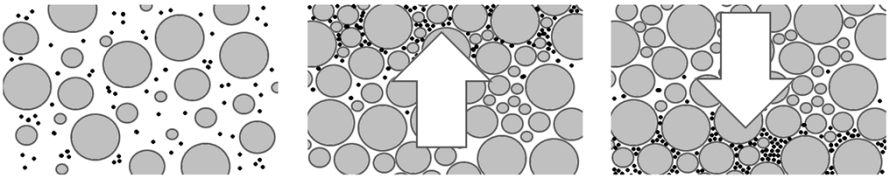

Figure 6. The image to the left shows pigment particles, here represented by grey circles, before immobilization. Depending on the material properties and/or drying conditions, dewatering can take place by evaporation (centre image) or by absorption (right image). Small latex particles, represented by black dots, tend to follow the aqueous phase after immobilization of the pigment particles.

When latex accumulates at the top of the coating structure, a reduction in gloss, and also a high print mottling can be observed. The reason is that the yellow-tinted latex film shrinks and forms a rough surface (Larsson et al. 2006; Preston et al. 2008)

The shrinkage of a latex film as a result of binder migration has been studied (Al-Turaif & Bousfield 2005). The addition of latex to the coating applied on both absorbent and non-absorbent (plastic film) substrates showed a reduced gloss, although the trend was, as expected, more obvious on the non-absorbent substrate. When a non-absorbent substrate is coated, no water can penetrate into the substrate. All the water thus has to leave the coating at the coating-air interface (centre image in Figure 6). It has been stated that both ATR-IR and SEM analyses are useful to obtain detailed information of the latex distribution (Kenttä & Pohler 2008). Results of such measurements have shown that coatings containing pigments with a broader PSD, and thereby a lower porosity, lead to greater latex migration towards the surface. The authors also noted larger areas of surface latex with increasing calendering temperature, but this was, as they explained, an effect of spreading rather than migration as the total amount on the surface remained the same.

In the case of thick coating layers, the latex migration is independent of coat weight due to filter cake formation (Zang et al. 2008). At low coat weights, a coating film may be immobilized mainly through water absorption by the base paper, and only a small amount of latex migrates to the surface. A heavier coat weight, on the other hand, contains more water which allows more extensive migration towards the surface. When a certain amount of latex has migrated to the surface, the filter cake will hinder further particle movement, and a heavier coat weight will not increase the amount of latex accumulated at the surface.

2.3 Thickeners

Thickeners are added to coating colours mainly to adjust the viscosity, but thickeners also act as co-binders and are often added together with latex to achieve both optimal viscosity and binding efficiency. Different amounts or different kinds of thickener can also affect the properties and the appearance of the coated surface, such as its oil resistance and gloss (Dean 1997).

The most commonly used thickeners are either synthetic, such as polyvinyl alcohol (PVOH), or organic, such as starch or carboxy methyl cellulose (CMC). The amount and type of thickener is an important factor affecting the latex migration

(Kugge 2004). Water-soluble thickeners form a gel-like structure in which the small particles are distributed, while synthetic thickeners accumulate around the pigment particles, thus allowing latex migration to a greater extent. PVOH has the capability of binding only the water in the region closest to the pigment particles, leaving the rest of the water more or less unchanged. CMC, on the other hand, binds the water more homogeneously and thus enhances the water retention of the coating colour.

A study (El-Sherbiny & Xiao 2005) has shown that thickener adsorption onto pigments results in a more viscous coating colour. Up to a certain point, this will lead to a greater fibre coverage and a smoother and more uniform surface. When the viscosity of the slurry increases further, the application of the coating is more difficult, and as a result the surface structure becomes uneven. The study also concluded that, compared with clay, GCC pigments appeared to be less sensitive to the type of thickener due to its limited interaction with the other components.

2.4 Coating techniques

Several techniques are used in the industrial coating of paper and board, and the demands for higher quality and faster production speeds, mean that old and new techniques are constantly being developed (Emilsson & Veyre 2009; Bohnenkamp et al. 2005; Kramm & Mair 2010). The coating process can be broken down into three operations: application, metering and drying. Applicator rolls and jet applicators, both illustrated in Figure 7, are the two application techniques that are the most common within the paper industry today.

The applicator roll transfers the coating colour from a trough to the substrate. Because of the direct contact with the coating colour, the system is also called a dip coater. A larger backing roll supports the substrate, and the amount of coating colour transferred depends on the distance to the applicator roll. The amount of coating transferred to the substrate is also determined by the viscosity of the coating colour and by the speed of the applicator roll.

A jet applicator, the right-hand image in Figure 7, applies the coating colour through a nozzle. The amount of coating colour is in this case controlled by the width of the slot, the jet pressure and also by the angle of the applicator to the moving paper web.

In both cases, as shown in Figure 7, a metering device located after the applicator removes excess coating colour and transfers it back to the re-circulation system. The two most commonly used technologies are blade metering or rod metering. A

blade can be either stiff or bent and is typically made of steel or ceramic. A stiff blade is static and does not adapt to the roughness of the paper, whereas a bent blade follows the structure of the substrate and hence creates a smoother surface. However, a bent blade is more likely to cause defects, such as blade scratches, due to wear of the softer blade material. Rod metering has been used for a long time in the paper coating industry. Instead of a blade the technique uses a wire-wound rod that either is stationary or rotates in the opposite direction to the moving paper web. As with the bent blade, the rod metering produces a smooth coating surface that follows the unevenness of the paper surface. A rod is also less likely to cause a web break when a thin and fragile paper substrate is coated (Dean 1997).

The coated paper is dried by means of air or infrared (IR) dryers, placed soon after the coating station. However, the coating colour starts to dry immediately after its first contact with the substrate, mainly because of water absorption into the paper but also due to water evaporation from the surface. To maintain the dimensional and strength properties of the paper, the time for water absorption must be kept as short as possible. IR dryers are more commonly used than air dryers because they remove water more rapidly with greater efficiency. IR radiation heats the water throughout the coating layer and can therefore be used to control the properties of the final coating layer (Fujiwara et al. 1989).

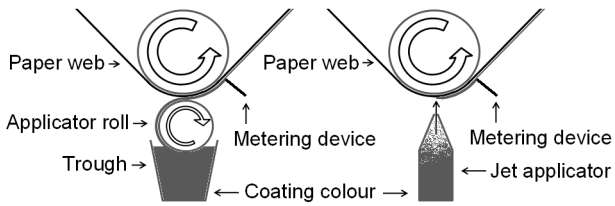

Figure 7. The two most common application techniques. To the left, the applicator roll that transfers the coating colour from the colour trough to the substrate, and to the right, a jet applicator that applies the coating through a nozzle. In both cases a metering blade or rod is used to control the coat weight.

For laboratory purposes, a bench coater is normally used. The coating speed for a bench coater is considerably lower than that used in industrial application, but the equipment is easy to handle and very suitable for laboratory trials. The bench coater uses a wire-wound rod (Figure 8), much like the rod metering principle described above, which is placed on top of the substrate. The rod is attached to a holder that moves the rod over the substrate at a given speed. The coating colour,

which is applied manually in front of the rod, is transferred to the substrate through the gap between the wire and the surface, while the excess coating colour is pushed forwards by the moving rod. To achieve different coat weights, rods with wires of different diameters are available. A broader wire diameter gives a wider gap for the coating colour to pass through, and this results in a thicker layer or a higher coat weight. After the application, the coated substrate can be dried freely under ambient laboratory conditions, by means of an infrared dryer or in an oven for a suitable time.

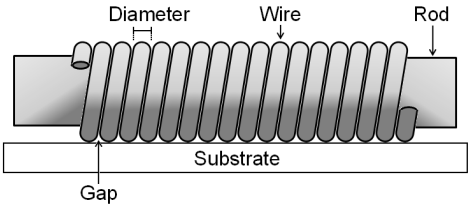

Figure 8. The principle for a bench coater with a wire-wound coating rod. Coating colour is applied in front of the rod, and when the rod moves over the substrate, a well-defined amount of coating colour is applied through the gaps. The thickness of the coating layer is controlled by the diameter of the wire.

2.5 Calendering of coated substrates

To increase the gloss and to improve the printability even further, coated materials are often calendered. During calendering, the substrate is compressed between two rolls and this decreases the roughness of the surface. One or both of the rolls can be heated, and a higher temperature or a higher line load increases the compression (Larsson et al. 2007). A negative consequence of this treatment is that the opacity and brightness of the coating layer decreases. The bulk and mechanical properties such as the tensile strength of the substrate also decrease (Endres & Engström 2005) and for this reason, the calendering is often performed at lower line loads when strength is critical. Studies have shown that the effects of calendering, such as increased gloss and decreased roughness, are influenced more by the temperature than by the line load (Park & Lee 2006). A certain deformation can be reached at a lower line load during calendering if a higher calendering temperature is used (Rättö & Rigdahl 2001).

The contact in the calender nip, i.e. the contact between two cylinders with parallel axes, can be described using Hertz contact theory:

$$p = \left(\frac{E \cdot F}{\pi L R} \right)^{1/2} \qquad [1]$$

where p is the maximum pressure, E is the elasticity modulus, F is the applied force, L is the cylinder length and R is the effective radius, which is a relationship between the radii of the two cylinders.

Calendering is usually performed using either a soft nip or a hard nip. A soft nip uses one steel roll and one polymer-coated roll. The polymer roll adapts to the local thickness variations of the paper, such as fibre flocs, and the pressure then becomes more evenly distributed. A hard nip uses two steel rolls which not only increases the total compression but also deforms the paper unevenly because of local thickness and bulk density variations.

The calendering speed also affects the result. A study using calendering speeds from 500 to 2200 m/min showed that when the calender speed was increased the roughness increased and the gloss decreased, compared to the effect of calendering at a lower speed (Lamminmaki et al. 2005). On the other hand, raising the temperature from 56 to 200 °C led to an increase in gloss and a decrease in roughness.

2.6 Optical and structural properties of coating layers

The optical properties of a coated material are dependent both on the overall structure of the coating and on the separate properties of each component in the layer. The surface roughness, the light absorbing and light scattering properties of the different components, the shape of the pigments and the coating porosity are examples of properties that will affect the total light reflection from a surface (van de Hulst 1981). The illumination source, or the wavelengths of the incident or incoming light has a huge impact on the resulting reflection. For example, a white surface ideally reflects all the incoming wavelengths equally, so that in normal sunlight that contains the whole range of visible wavelengths, the surface appears white. If only one wavelength, or a narrow range of wavelengths is used in the illumination source, the surface looks different. It can then appear completely blue or red as illustrated in Figure 9. For this reason, illumination conditions are standardized and different illuminations are used for different measurements (Pauler 1999).

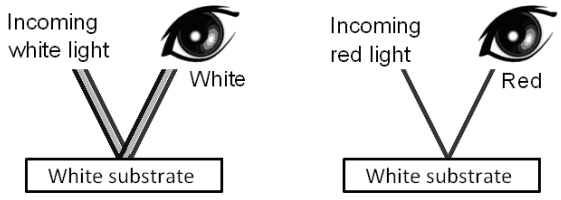

Figure 9. When white light, containing all the visible wavelengths, is reflected from a white surface, we see it as white (left-hand image). However, if the same white surface is illuminated with only a narrow range of wavelengths, for example red light, the surface appears red (right-hand image).

The human eye and brain are outstanding instruments, and the way in which we judge the appearance of a surface and see the light reflections can probably never be imitated by any measuring device (Kuehni 1997; Berns 2000). The reception of a light stimulus by our visual system is a very complex process that involves the cells in our eyes, optic nerves and visual areas in the brain. Due to cultural diversity, images and colours may be interpreted differently by different people, so that we can never properly describe a vision to another person. However, to standardise optical measurements, a wide range of instruments that monitor different optical properties have been developed and the measurement conditions have been standardized.

2.6.1 Gloss

Light can be reflected from a surface either diffusely or directionally. The light reflection giving rise to the perception of gloss is directed reflection, also called specular or mirror reflection, and a high gloss is often desired when a paper product, printed or unprinted, is produced. A high gloss makes the product, for example a packaging, look more elegant and expensive. In some cases, more effort and resources are actually concentrated to the manufacture of the package than to the contents themselves. The gloss is closely related to the surface roughness, and for coated paper, it has been shown that gloss is predominantly governed by the surface texture of the paper (Caner et al. 2008).

The gloss, expressed as a percentage, is defined as the amount of light that is reflected from a surface at the same but opposite angle to the normal as the incident light. The most commonly used incident and viewing angles within the paper industry are 75, 60 and 20°, where smaller angles are most suitable for highly glossy samples. The equipment for measuring gloss is very user-friendly and the

measurements can be made quickly, and for this reason the gloss is usually measured at a single angle, even though the number of viewing angles in reality is infinite when a person looks at a surface. To obtain a wide range of reflections at different angles, equipment such as a goniophotometer has been developed, where not only the viewing angle but also the illumination angle can be altered. The results obtained from such equipment give much more detailed information about the optical properties of the surface, but because of high costs and more time-consuming measurements, the technique has not become widely used in the industry. However, alternatives are sometimes suggested. A simple equipment called a micro-goniophotometer, based on an inexpensive video camera and simple optics, has been investigated (Arney et al. 2006). It has been shown to produce significantly more information than that given by standard gloss measurements. The authors presented plots of a bidirectional reflectance factor distribution function (BRDF) that were related quantitatively and directly to Fresnels law of specular reflection, to surface roughness and, in some cases, to subsurface effects. A standard gloss measurement does not distinguish between these effects.

Figure 10 illustrates the gloss of three different surfaces. The image to the left represents almost zero gloss. The surface in this case is very rough and porous, and the light is reflected equally in all directions, i.e. the reflection is diffuse. A perfectly diffuse reflection is called Lambertian reflectance after Johann Heinrich Lambert (1728-1779), a Swiss physicist. In reality, Lambertian reflectance is difficult to achieve, but the concept is useful when surfaces are studied and simulated and assumptions about unknown properties are to be made.

The central image in Figure 10 shows a semi-glossy surface. A large part of the incident light is specularly reflected, but a large part is also reflected diffusely. This is the case, more or less, for all paper products where the surface roughness is low but large enough to affect the light. At a measurement angle of 75°, the gloss is roughly 1-10% for uncalendered and uncoated papers, 15-30% for calendered uncoated papers and 30-80% for coated and calendered papers (Pauler 1999).

The right-hand image in Figure 10 shows a perfect specular reflection. For a paper product this situation is impossible to achieve, and only mirrors and highly polished surfaces of for example steel can reach this stage (Pauler 1999).

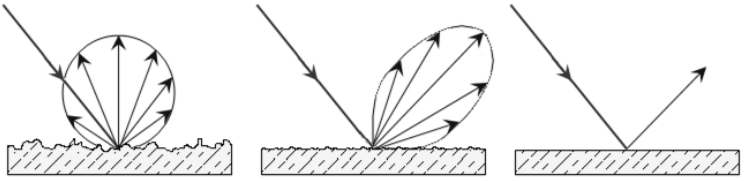

Figure 10. Three types of gloss. Diffuse reflection to the left, semi gloss in the centre and total gloss or perfect specular reflection to the right.

2.6.2 Brightness

The brightness is defined as the intrinsic diffuse reflectance factor, R_∞, at an effective wavelength of 457 nm, R_{457}, and is measured using a diffuse light source. R_∞ is often described as reflection against a background of an "infinitely thick pad of papers", but in reality a sufficiently large number of paper sheets, so that doubling the number of sheets does not affect the outcome, is used.

If only a few samples are available, R_∞ can be calculated using a two-background method:

$$R_\infty = a - (a^2 - 1)^{1/2} \qquad [2]$$

$$a = \frac{1}{2} \cdot \frac{(R_{gw} - R_{gs}) \cdot (1 + R_w \cdot R_s) - (R_w - R_s) \cdot (1 + R_{gw} \cdot R_{gs})}{R_s \cdot R_{gw} - R_w \cdot R_{gs}} \qquad [3]$$

where R_{gs} is the reflectance factor of the black background, R_{gw} is the reflectance factor of the white background, R_s is the reflectance factor measured on one sheet against R_{gs} and R_w is the reflectance factor measured on one sheet against R_{gw}. The equations are based on the Kubelka-Munk theory, further explained below, and their use were described in detail by (Karipidis 1994).

The spectrophotometer is a device that measures the diffuse reflectance factor and can therefore be used to measure brightness according to standardised methods (ISO 2470). From the results of the measurements, opacity, light scattering and light absorption, further discussed below, can be calculated. The spectrophotometer method standardized within the pulp and paper industries is based on the d/0° geometry, where the d stands for diffuse illumination, and 0° means that the measurement is made perpendicular to the sample.

The spectrophotometer (Figure 11) consists of a sphere that is coated with white pigment on the inside. The light sources are shielded to prevent any direct light reaching the sample, which is placed at the bottom of the device, and is thus illuminated entirely with diffuse light reflected from the walls. The detector is placed at the top of the sphere, and is shielded by a gloss trap whose purpose is to prevent any light specularly reflected from the sample from reaching the detector.

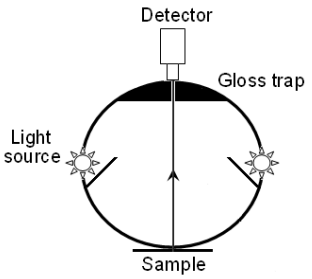

Figure 11. The spectrophotometer for measuring of brightness, based on the d/0° geometry.

The reflectance factor can also be measured by means of a 45°/0° geometry, where the sample is illuminated at an angle of 45°. The advantage is that gloss can be screened off more efficiently. Disadvantages are that the structure of the sample affects the measured reflectance factor and the results obtained differ from those obtained using the d/0° geometry. The 45°/0° geometry is often used within the graphic arts industry, and for this reason the results of optical measurements made by paper makers using the d/0° geometry, are not always accepted by the printers. A more general model designed to describe optical properties in a more correct way, like the DORT2002 described in section 5.2, is an attempt to solve this problem.

2.6.3 Opacity

Opacity is a property that describes the proportion of light transmitted through a material or a surface. When the opacity decreases, the material becomes more transparent.

In the paper industry, the opacity is calculated from the reflectance factor of a single sheet against a black background, R_0, and the reflectance factor of an opaque pad of papers, R_∞, and is expressed as a percentage:

$$Opacity = \frac{100 \cdot R_0}{R_\infty} \quad [4]$$

For coating layers, the opacity typically increases with increasing coat weight, and with increasing amount of plate-like pigments, such as kaolin clay. Coated surfaces with high light scattering in general give high opacity.

2.6.4 Refractive index

The refractive index of a material is defined as the ratio between the speed of light in vacuum and the speed of light in the material. It is expressed as:

$$n = \frac{c}{v} \quad [5]$$

where n is the refractive index, c is the speed of light in vacuum and v is the speed of light in the material. Since c is always equal to or greater than v, the value of n for a material is always equal to or higher than 1.

Figure 12 explains the basic principle of the refractive index. The incident light, coming from a medium with refractive index n_1 towards a material with a higher refractive index, n_2, has a certain angle to the normal (θ_i). When the light reaches the surface, part of it will be reflected from the surface at the same, but opposite angle from the surface (θ_r). The remaining light will be transmitted through the surface into the material at a smaller angle to the normal (θ_t). The higher the refractive index for the material, the smaller will θ_t be. In other words, if n_2 increases θ_t will decrease.

The refractive index of a coating layer has a strong impact on its optical properties. A higher pigment refractive index will lead to a smaller transmission angle, as shown in Figure 12. Air has a refractive index very close to 1, while pigments like GCC and kaolin clay have values of 1.5 – 1.6. Pigments with a very high light scattering capacity, like titanium dioxide or zinc oxide, have refractive indices between 2.0 and 2.6 (Pauler 1999).

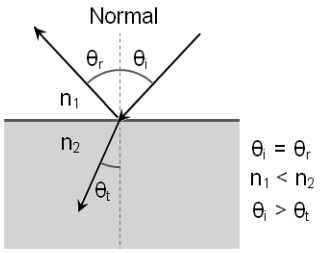

Figure 12. When light travels from a medium of lower refractive index (n), to a medium of higher n, the angle of transmission (θ_t) becomes lower than the angle of incident light (θ_i), that is, if $n_1 < n_2$ then $\theta_i > \theta_t$. The angle of surface reflected light (θ_r) is always equal to θ_i.

The effective refractive index of a porous coating layer is a combination of the individual refractive indices of the coating material and the entrapped air. As shown in Figure 13, the effective refractive index depends on the proportions of air and coating material in the surface of a coating layer. If the micro-roughness decreases after, for example, calendering, less air will be present in the surface layer and a more dense coating surface is formed, which will result in an increase in the effective refractive index.

Figure 13. A porous structure (left), in this case the top surface of a coating layer, contains both coating material and air. The two components with their individual refractive indices can be modelled as one layer (right) with an effective refractive index that depends on the relative proportions of the two components.

2.6.5 Surface topography and porosity

A surface is a well-defined two-dimensional boundary between two media, for example a solid material and air. When a paper surface is observed it appears to have a very smooth and flat surface, but in close up it is rough with numerous "peaks" and "valleys". The roughness can be divided into three categories according to size : optical roughness on a length scale < 1 μm, micro-roughness at 1 – 100 μm and macro-roughness on a length scale > 0.1 mm (Niskanen 1998). In the case of coated papers, pigment surfaces form the optical roughness while the pigment shape creates the micro-roughness. In general, roughness on the scale close to or less than the wavelength of light is often regarded as micro-roughness.

Macro-roughness is mostly associated with the fibre structure in the paper substrate. This range of structures describes an almost fractal pattern, and on a small scale the surface of a coating layer can be regarded as being infinitely large. However, in the paper and coating industry, the optical roughness and sometimes also the micro-roughness are on too small a scale when the surface roughness is to be determined.

Surface roughness can be measured in several ways. Figure 14 demonstrates two methods: peak-to-valley height and average deviation from a reference surface. The peak-to-valley method is very sensitive to single peak features, while average deviation is less sensitive to such local extreme values due to the averaging.

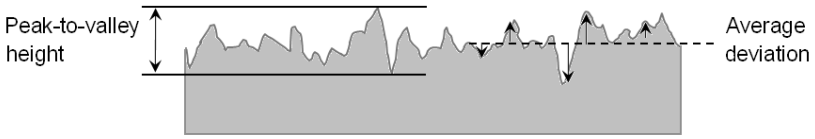

Figure 14. The roughness of a paper surface. Roughness can be expressed as peak-to-valley height or average deviation.

A quick and common way to measure the surface roughness is by an indirect air-leak method such as the Parker Print Surf (PPS) method. A measuring head is pressed against the paper sample, and the rate of flow of air that is forced through the space between the sample and the measuring head is recorded. This means that the air flow decreases with decreasing roughness. The PPS method recalculates the air flow to an average roughness value expressed in μm.

A coating layer is also characterized by its porosity. As has been mentioned in section 2.1, different shapes and sizes of pigments create different particle size distributions, which in turn affect the size and shape of the pores formed in the consolidated coating layer. When the porosity of a surface is explained and calculated, the pores are often described as tubes of a fixed diameter that stretch vertically from the surface and downwards through the coating layer. This is of course a rough simplification, but for GCC coatings it is often a sufficient assumption. However, clay coatings produce more complex pore structures, where not only the size and shape but also the orientation of the pores must be considered. A blend of clay and GCC particles often creates a packed structure with a low porosity. (Chinga et al. 2002) have shown that coatings containing a larger proportion of clay produce a lower pore area fraction than a coating

containing less clay. It was also shown that a coating layer containing either a high or a low proportion of clay, had a more compressed structure at the surface than inside the coating.

It has been shown that calendering can lead to smaller pore openings, or so-called closed areas, on the surface of coated paper (Chinga & Helle 2003). The lack of these closed areas on uncalendered surfaces indicates that they were not caused by drying or any other treatment. These areas have been found in low coat weight regions and are characterized by local variations in smoothness and gloss (Xiang et al. 2000). It has been suggested that the local variations may be caused by a greater binder content, but other studies have found no such differences (Xiang et al. 2000). The closed areas have also been shown to affect the print mottle. It was also suggested there was a correlation between the size of the closed areas and print mottle (Chinga & Helle 2003).

Polarized light reflectometry and its application in the study of paper coating structure and optical properties has been described in detail by (Elton & Preston 2006b). It is a fast measurement process that produces a large amount of data including micro-roughness, macro-roughness, surface porosity, refractive index and gloss. All the information is obtained from a single, non-destructive, measurement taking about 0.5 seconds.

(Elton & Preston 2006a) presented results from measurements using polarized light reflectometry. They found the analysis of the effective refractive index to be an indirect method for determining pore size within a coating layer, although the data for pore volume was more scattered than for pore diameter. They also found that a good correlation exists between the micro-roughness of a GCC coating and the effective refractive index, indicating the importance of pigment packing at the surface. Measurements were made on calendered paper sheets to probe the changes in surface topography, and it was found that the first few nips decreased the macro-roughness due to smoothing of the base paper. Further nips did not affect the base paper, but the gloss increased due to a decrease in micro-roughness in the pigment coating.

3 Printing

Printing is a process for the mass production of text or images by means of a printing press. Several printing techniques are in use. The oldest is the letterpress technique, from which all modern printing processes have developed. Letterpress uses a relief pattern, a mirror image of the intended image where ink is positioned. When the pattern is pressed against a paper sheet, an image is produced and this can be repeated numerous times. Although Johann Gutenberg is said in western society to have invented the letter press in the middle of the 15th century, simple printing techniques were used in Asia already about 1000 years earlier.

As in the case of paper surfaces and coating layers, printed areas both absorb and scatter light. However, compared to white surfaces, the light scattering is low due to a more homogeneous refractive index, and the light absorption is high. The function of a printed surface is to absorb light of certain wavelengths and to reflect only the desired colour. The absorbed energy may however cause chemical reactions leading to colour changes and fading.

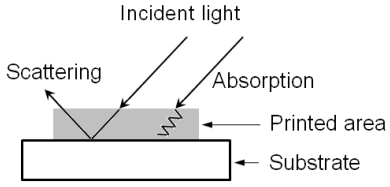

Figure 15. Behaviour of light in and around a printed area.

Because of the low amount of scattering in the printed areas, the light travels relatively un-scattered through the ink and is scattered when it hits the substrate below. Light that is reflected from layers in the print or from the substrate underneath will consist only of the wavelengths that are not absorbed and hence the printed area is perceived to have the desired colour (Figure 15). However, light scattering occurs in all directions, and light that is scattered sideways, beneath the print is lost and this creates a "shadow", making even the finest printed dot look out of focus, and the effect is called optical dot gain, a phenomenon further discussed in section 3.6.3.

3.1 Flexography

Letterpress was the dominating printing technique for centuries until other methods, mainly lithographic offset printing, were developed. Like the old

movable type, the letterpress uses relief printing elements, but the image that is to be printed is nowadays made out of a single metal plate. The plate is attached to a cylinder in the printing press. The ink is distributed to the printing plate via a system of rollers, and the substrate is printed when it passes between the printing plate and an impression cylinder. Letterpress using hard printing plates is still in use today, but mainly for products that do not require a high print quality, as for example paperback books and telephone catalogues.

Like letterpress, flexography is a relief process, but the plate is made of photopolymer or rubber to give a flexible contact with the substrate, which makes it possible to print rough and uneven surfaces. The principle of the flexographic printing process is shown in Figure 16. From the ink reservoir, the ink is picked up by the anilox roll which is engraved with a pattern of cells that control the amount of ink needed for a certain plate or print quality. A doctor blade scrapes off the surplus, and the remaining ink is then transferred to the plate cylinder.

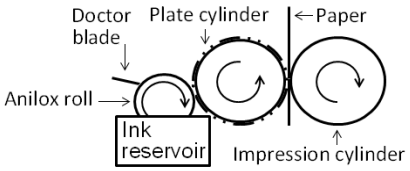

Figure 16. The principle of flexography. The ink is picked up by the anilox roller where a doctor blade removes the surplus. The ink is then evenly distributed to the raised region on the plate and finally to the paper.

Apart from rough surfaces, such as corrugated paperboard, flexography can be used to print on a broad spectrum of substrates such as plastic, metallic films, cellophane and paper, and the technique is often used in the packaging industry. One of the weaknesses of flexography is the increasing cost for the production of plates as the technique evolves.

3.2 Flexographic presses

Flexographic presses can be roughly divided into four sections; the unwind section, the printing units, the dryers and the rewind section. In a linear press (Figure 17), the sections are arranged in series. The substrate is unwound prior to entering the first printing unit and then passes the first dryer before entering the next printing unit. This cycle is repeated until the printing is completed and the substrate is reeled up in the rewind section. The printing units are movable and the order in

which the different colours are printed can be changed. The substrate can also pass a printing unit without being printed to allow a longer drying time. Figure 17 shows a linear press with six printing units. Ten or more units can be lined up in a commercial press. The dryers can be of the hot-air or infrared type. Radiation curing by ultraviolet light and electron beam curing are also possible.

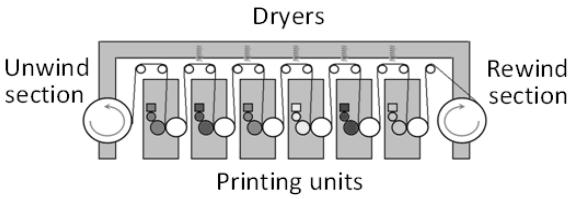

Figure 17. Linear press. The substrate is unwound, fed into the first printing unit and then into the first dryer. This cycle is repeated until the substrate reaches the rewind section.

The design of the linear press is very practical for printing operators. All the sections are located on the ground level and this make it easy when upstart and adjustments are to be done. It is important that the web tension is well controlled in the unwind and rewind sections, not only to avoid wrinkles and breaks during the process but also to avoid mismatching or misregister of prints from different sections.

To avoid these disadvantages other kinds of flexographic presses have been developed. The image to the left in Figure 18 shows a stack press in which the printing units are placed vertically, thus reducing the required floor space. On the other hand, the arrangement makes the press more difficult to handle for the operators with the units out of reach from ground level, and the risk of misregister remains. To minimize, or even completely eliminate the risk for misregister, central impression presses, or simply CI presses, have been developed. As can be seen in the right-hand image in Figure 18, the printing units in the CI press share a common impression cylinder. Since the substrate is in contact with the single impression cylinder, its velocity remains the same between the printing units and misregister is thereby avoided.

Figure 18. To the left, a stack press where the printing units are placed vertically, and to the right, a CI press where the printing units share a common impression cylinder.

As in the case of the linear press, it is possible to remove or switch the location of each printing unit in both the stack and the CI press.

3.3 Printing plates

The first flexographic printing plates were made of rubber. Even though some rubber plates are still in use, the most common ones these days are made of photopolymer. Figure 19 shows a flexographic printing plate viewed from the side. The jagged surface represents the relief pattern, and the raised parts, the face, forms the image area. The relief depth varies between plates, but is typically about 0.4 mm. The total plate thickness is usuallt 3 – 6 mm, but the trend is towards thinner plates.

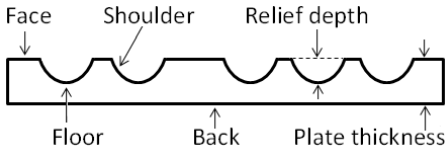

Figure 19. The parts of a flexographic printing plate.

As the name implies, photopolymer plates are made of light-sensitive polymers. The polymers are soluble in organic solvents, but on exposure to ultra violet (UV) radiation, a cross-linking process takes place and makes the exposed areas insoluble. There are many different systems for the production of photopolymer plates, but they can roughly be divided into two major techniques: conventional and digital procedures.

The conventional process is shown in Figure 20. As a first step, the photopolymer plate undergo back exposure. The time and intensity of this UV treatment determines the floor thickness, which in turn controls the relief depth. In the second step the face side, covered with a film negative under a vacuum cover

sheet, is treated. The film negative is coated with a black film, and only the image area is transparent. The polymer plate is thus exposed to light only on the image area where the polymer cross-linking takes place.

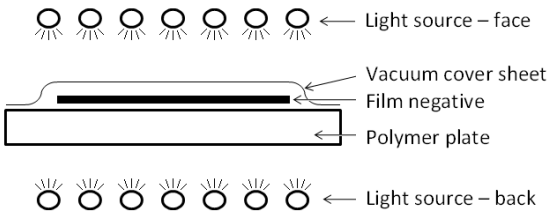

Figure 20. The conventional way of exposing a photopolymer plate to produce an image.

After the UV treatment, the non-image areas are still soluble and are easily dissolved in an appropriate solvent. The residual material is then brushed away, and a drying and resting time of several hours follows. Finally the plate undergoes a finishing process, usually by yet another UV treatment, to give a well-defined surface. The digital process follows the same procedure as the one described above, but no negative film or vacuum cover sheet is then required. The photopolymer plate is coated with a carbon-based material which is removed from the image areas by a laser beam.

The hardness of a printing plate can be varied depending on the substrate properties. This is measured by means of a Shore hardness tester. A needle is pressed against the printing plate and the deformation of the material is measured. The unit for hardness is expressed as °Shore A, and the value increases with increasing plate hardness (Kipphan 2001). It has been shown that a soft printing plate of 64° Shore A transferred more ink to the substrate and produced prints of higher print density and less dot gain than a harder printing plate of 75° Shore A (Johnson et al. 2003).

3.4 Anilox rolls

Controlling the amount of ink transferred to the substrate is fundamental in all printing processes. As small an amount of ink as possible should be used, not only because of the costs of the ink itself, but also to shorten the ink drying time and hence speed up the printing process. Another reason for minimizing the ink amount is to reduce dot gain that would lower the print quality. In the 1930's, a new way of transferring ink to the flexography rubber plate was developed. A

cylinder known as the anilox roll, engraved with a fine pattern of cells, distributes a controlled amount of ink to the printing plate. The anilox roll is engraved with cells of equal shape and size as shown in Figure 21. The most common anilox rolls are ceramic-coated steel rolls. The thickness of the ceramic layer is about 0.25 mm, and the cells are burned into the layer by means of laser.

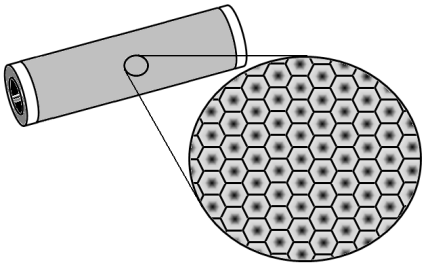

Figure 21. Engraved cells on the anilox roll. The cells in the picture are hexagonal in shape, but other forms also exist.

Different sizes and shapes of the cells make it possible to transfer different amounts of ink to the printing plate. It is important to choose the most suitable anilox roll for a specific print product. The finer details that are to be printed, the less ink should be transferred to the plate. The amount of ink that can be carried by a specific anilox roll is defined by the number of cells per centimetre and the volume or depth of the cells. A cell count of about 80 cells per centimetre can be considered coarse, while a cell count of about 300 cells per centimetre can be described as fine. The depth of the cells, or their volume, is also an important property. A fine cell count can carry more ink than a coarse one if the finer one has a larger cell volume.

The cell volume is defined as the volume of the total number of cells on an area of 1 m^2, and is expressed in cm^3 or ml. The cell volume for an anilox roll can vary between 2 and 8 cm^3/m^2. It is important to remember that this volume describes the ink that the anilox roll carries, and not the amount that is actually transferred to the printing plate and the substrate. It has also been shown that the ink formulation can affect the amount of ink transferred to the substrate (Rentzhog & Fogden 2005).

In the early flexographic printing systems, the ink was transferred to the anilox roll via a fountain roll. This system made it difficult to control the ink quantity and the printing plates often became clogged, which resulted in blurred images. When the

doctor blade was introduced, the amount of ink transferred from the anilox roll to the printing plate could easily be controlled. The doctor blade can be either positive or negative with respect to the tilt angle against the anilox roll (Figure 22). A negative blade is more efficient in the removal of excess ink, but it also wears the equipment more rapidly.

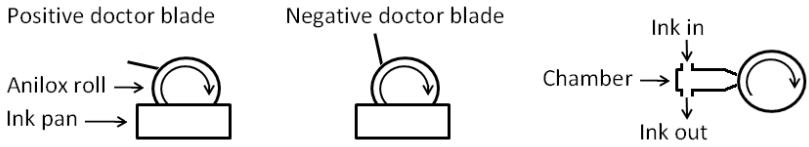

Figure 22. The doctor blade can have a positive, left image, or negative, centre image, tilt angle. The chamber system, on the far right, consists of both a positive and a negative doctor blade.

More common is however an enclosed or chamber system that is now standard of all flexographic printing presses. Instead of an open pan the ink is held in a tank and is led to a chamber located beside the anilox roll. In the chamber, which is equipped with one positive and one negative doctor blade, the ink is applied to the anilox roll. The surplus ink is then led out back to the tank. With the closed chamber system, it is much easier to keep both the ink and the surrounding equipment clean. Evaporation of solvent and resulting changes in the properties of the ink can also be avoided.

3.5 Flexographic ink

Inks for flexographic printing are either solvent-based, water-based or of the UV curing type. For environmental reasons, the water-based inks have undergone a major development since the 1980´s, but for the same reason, the most recent growth has been in UV-curable inks.

Printing ink consists of four main ingredients: a pigment, a binder or resin, a solvent or water and various kinds of additives. 10 to 15 weight percent of the ink consists of pigment. White inks have a higher pigment content, 30 to 35 weight percent, to give acceptable opacity. The colour is either in the form of soluble dye or an insoluble pigment. The pigment is originally rough and must be ground into tiny particles that are insoluble in the solvent and are kept in suspension by the resins. The size and shape of the pigment and resin particles have a major impact on the final print quality. Small particles give a good coverage, and smooth ones result in a high print gloss. The refractive index of the ink layers is approximately

the same magnitude as that of the coating pigments, i.e. about 1.5 – 1.6. However, the refractive index of a light-absorbing ink layer is more complicated to estimate than that of a white and nearly non-absorbing coating layer. More generally equation [5] can be written as:

$$n_c = n + ik \qquad [6]$$

where n_c is the complex refractive index, n is the real part of the refractive index and k is the absorption loss as the light travels through the material. Several studies have been carried out to determine the complex refractive index for printed layers (Peiponen et al. 2008; Bakker et al. 2004; Niskanen et al. 2007; Preston & Gate 2005). For practical reasons, smooth samples applied on flat materials without any roughness or porosity are often used in such studies, and the impact of the roughness of a real printed substrate on the complex refractive index is often discussed. However, it has been indicated that the scale of roughness only marginally influences the measured refractive index of a printed surface (Preston & Gate 2005).

As mentioned above, one of the functions of the resin is to keep the pigment suspended in the solvent, but the resin is also important for the solvent retention, and thus the final optical properties, of the print. The resin attaches the pigment to the substrate and represents 10 to 20 weight percent of the ink. The resins must be soluble in the solvent, and are therefore selected on the basis of their solubility in the solvent in question. In water-based inks, the resin is typically acrylic solution polymer and acrylic emulsion. The resins must totally cover the pigment particles to suspend them in the fluid. When the ink is transferred to the substrate, the solvent evaporates or is absorbed by the substrate, and the resins starts to create inter-molecular chains and finally form a cross-linked network.

About 60 to 70 weight percent of the ink consists of solvent. Alcohols are conventionally used as solvents in solvent-based inks. A small amount of an alcohol is sometimes added to a water-based ink to speed up the drying. To control the drying rate, propylene glycol is used in both water-based and solvent based inks. The drying rate of the ink strongly affects the ink setting and the print quality, and it is therefore important to optimize the inks with respect to the substrate to be printed on. The ink viscosity is controlled by the amount and nature of the solvent. Viscosity affects the ink transfer from the anilox roll to the printing plate and to the substrate, as well as the flow through the chamber system.

The viscosity (η) describes the flow properties of matter, and it is defined as:

$$\eta = \frac{\tau}{\dot{\gamma}} \qquad [7]$$

where η is the viscosity, τ is the shear stress (force required per unit area to the deformation velocity) and $\dot{\gamma}$ is the shear rate (velocity).

A suitable way to measure the rheological response of coating colours and printing inks is by means of a rotational viscometer, since the response changes as a function of shear rate (Larson 1999).

The shapes of the particles influence the viscosity of a suspension. Spherical shapes usually generate a lower viscosity than irregular or plate-like ones, due to the interaction between the particles. The viscosity of a suspension also depends on the particle size and particle size distribution. Small particles tend to give a suspension with a higher viscosity than do larger particles. This is due to the fact that a larger surface area creates more inter-particle bonds. At low shear rates, chemical factors, mostly van der Waals attractions, affect the viscosity. At high shear rates, where the bonding between the particles is broken by the high shear, the hydrodynamic effect is the major factor affecting the viscosity. Under these circumstances, small and spherical particles act as lubricants. Smaller particles reduce the viscosity more than larger ones. A typical behaviour of a shear-thinning fluid is shown in Figure 23. The viscosity is relatively high at a low shear rate and decreases when the shear rate increases.

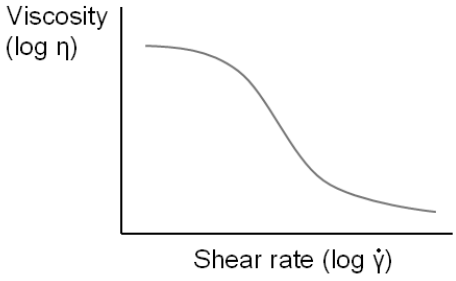

Figure 23. An example of a viscosity curve of a shear thinning fluid.

Temperature also has an influence on the viscosity. The higher the temperature, the lower is the viscosity. Another factor that affects the viscosity is the surface

charge of particles. Surfaces with the same sign increase the repulsive forces and the viscosity decreases. Oppositely charged surfaces on the other hand can lead to aggregates with a higher viscosity as a result. Finally, the solids content of the suspension is an important factor affecting its viscosity. In a given volume, the distance between particles decreases with a higher solids content, and hence it becomes more likely that they will interact with each other.

For printers, a rotational viscometer is a time-consuming and impractical equipment, and although they are not as accurate as a rotational viscometer, efflux cups are often used for viscosity measurements. A number of different systems are available, e.g. Afnor, Ford and Zahn cups, all being operated by the same principle, which is illustrated in Figure 24. The time until a given volume of liquid stops flowing through a specified hole is recorded, and the number of seconds is taken as a measure of the viscosity.

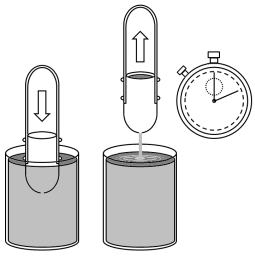

Figure 24. Viscosity measurement by means of an efflux cup. The cup is filled with ink, and the number of seconds it takes for it to flow through the hole in the bottom is taken as a measure of the viscosity.

The ideal viscosity is different for each printing press, and sometimes even for each printing unit in the same press and hence has to be optimized at each stage. The viscosity has a great impact on the print density. A high viscosity ink creates a more dense print as more ink is transferred (Walker & Fetsko 1955), i.e. a darker tone than ink of lower viscosity.

Additives, representing 0.5 to 10 weight percent of the ink, are added for several purposes. Wax or silicones are used to create a protective layer on top of the print. With slip compounds, the printed areas becomes smoother and more protected against wear when sheets are rubbed against each other. Plasticizers are added to make the print more flexible. Other additives such as antifoamers, friction compounds, surfactants and adhesion promoters can be added to facilitate the

printing process or to match the demands for specific properties of the printed surface. For water-based flexographic inks, pH regulators are particularly important as they regulate the speed at which the resin polymerizes.

3.5.1 Ink transfer and ink setting

As discussed in section 3.4, the anilox roll controls the amount of ink transferred to the plate and further to the substrate, but other factors also affect the ink transfer. When a substrate passes the printing nip, it becomes compressed (Figure 25) and the contact area between the substrate and the printing plate is dependent on the roughness of the substrate and the pressure in the printing nip. The ink then sets to the substrate, a process depending, among other things, on the viscosity of the ink and the porosity of the substrate. Finally, in the printing nip exit, ink splitting occurs when the contact area and the moving substrate separate. The factors already mentioned above, as well as the printing speed, affect the amount and the characteristics of the film splitting.

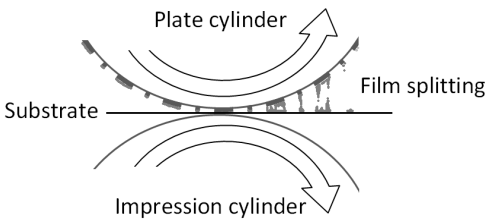

Figure 25. Ink transfer. When the substrate leaves the print nip, film splitting occurs.

A study has shown that a rough surface substrate accepts more ink than a substrate with a smooth surface. However, this is only valid for a certain degree of roughness. Too rough a surface reduces the contact area in the nip, and this reduces the ink transfer (De Grace & Mangin 1983). The study also concluded that the ink penetration increased to a certain extent with increasing nip pressure. Too high a nip pressure closes part of the surface pores and reduces the ink transfer.

An early equation for calculating the amount of ink transferred to the substrate was presented by Walker and Fetsko (Walker & Fetsko 1955):

$$y = (1 - e^{-kx})\left[fx + b(1 - f)(1 - e^{-x/b})\right] \qquad [8]$$

where y is the amount of ink transferred per unit area, x is the amount of ink on the printing plate before printing, k is a constant related to the smoothness of the

paper, b is the amount of ink that can be immobilized during impression and f is the fraction of ink that is transferred to the substrate during film splitting. More recent studies have suggested modifications of the original equation to make it valid for different kinds of coated surfaces (Walker 1980).

When the ink has been transferred to the substrate it should be adsorbed to the surface and dry, a process known as ink setting. Immediately after printing the ink solvent starts to evaporate and to be absorbed into the substrate, and the print is usually considered to be dry when the process has reached a point where the print is rub proof. The length of this time strongly affects the print gloss due to ink leveling. A slow ink setting produces a smooth ink surface whereas a rapid setting ends the leveling process before a smooth surface is reached, and this leads to a rough ink surface (Desjumaux et al. 1998; Gane & Ridgway 2009). Substrates coated with a pigment of broader PSD, which gives a lower coating porosity, result in a higher print gloss and a higher print density due to the lower ink penetration in the z-direction (Figure 26) (Preston et al. 2008; Ström et al. 2003).

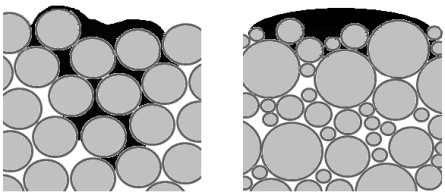

Figure 26. Figures illustrating ink penetration. To the left, a pigment with narrow PSD gives a higher penetration in the z-direction. To the right, ink covers more of the surface and gains higher gloss due to less ink penetration thanks to the more close-packed coating structure

3.6 Print quality

Images created by the print process often consist of both full-tone areas and half-tone areas. Producing solid ink areas is a rather straightforward process that places ink in a defined pattern, such as a letter in a text, onto the substrate. Half-tone areas are used to create light and dark tones of a colour. The illusion of shade is created by a large number of small dots of solid ink, as shown in Figure 27. If the dots are large or close together, the area will appear dark, and if the dots are small or wider apart, it will appear brighter. The image to the left has fewer lines of dots per centimetre than the image to the right, which makes it coarser with clearly visible dots. The number of lines per centimetre that an image should have depends on where and how it is to be displayed. Fewer lines per centimetre require

a greater viewing distance. More lines per centimetre, as in the right-hand image in Figure 27, are required for an image that is going to be viewed from a short distance. The reason is the limiting feature of the human visual system.

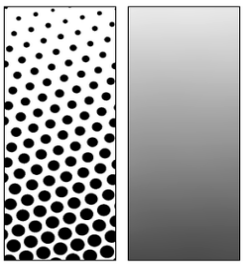

Figure 27. Half-tone images are used to create an illusion of dark and light areas.

The tone value is expressed as the size of substrate area that is covered with ink dots. 100 % tone value is equal to a solid ink area and 0 % is an unprinted substrate. The upper regions of the images in Figure 27 have a tone value of about 10 %, while the lower regions have a value of about 75 %. The dot size is different on the two images, but the tone areas are the same. In Figure 27 the dots are circular, but they can also be elliptical or square. Stochastic patterns, with random instead of lined-up dots, can also be used.

3.6.1 Print density

The optical print density, or the reflection density, is a measure of contrast. In other words, the property describes how well the substrate is covered by ink after printing. The print density is expressed as the logarithm of the relationship between the reflectance factors of the unprinted and printed substrate:

$$D_S = \log_{10}\left(\frac{R_\infty}{R_S}\right) \qquad [9]$$

where D_S is the print density of a solid tone, R_∞ is the reflectance factor of the substrate and R_S is the reflectance factor of the printed solid tone. In the same manner the optical print density can be determined for a half-tone print.

Up to a certain point, the print density increases with increasing amount of ink transferred to the substrate. However, after the point when the surface is

completely covered, and the ink layer is thick enough, the print density reaches a stable value that is not affected by additional ink (Tollenaar & Ernst 1962).

Print density is measured using a densitometer, shown in Figure 28. A printed sample is illuminated by white light at a certain angle. The light, after passing a collector lens, is reflected from the surface. The reflected light passes a polarization filter and yet another collector lens, and finally a coloured filter which allows only the desired wavelengths to pass.

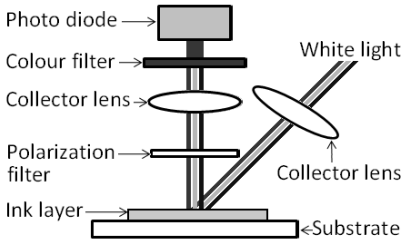

Figure 28. Densitometer. White light is reflected from a printed area. After passing a coloured filter, the detector can register how much light of a certain colour is reflected.

Due to differences in pigment shape the different inks have different coverage capacities, and thereby different reflection densities. In theory, the density can have values from 0 to 4, but the value is about 1.2 to 1.5 for cyan, magenta and yellow, and slightly higher for black.

3.6.2 Mottling

A substrate with local variations in density and surface energy often exhibits an uneven ink absorption. This effect, called mottling, appears as a speckled and uneven print and can be described as unwanted reflectance variations (MacGregor et al. 1994). The degree of mottling can be increased or decreased by changing the ink properties or by adjustment of the printing press, but the heterogeneity and the structure of the paper substrate are of major importance (Kipphan 2001). The reflectance variations of unprinted board, known as white top mottling, can in some cases be related to print mottle, but this relationship has been shown to be more distinct for uncoated than for coated paper (Sadovnikov et al. 2008).

It is difficult to judge mottling instrumentally and to quantify the result because the task is to evaluate what the human eye sees and how the brain interprets the image. For example, a periodic mottling is more obvious than a random one due to the

human sensitivity for detecting regular patterns (Lindberg & Fahlcrantz 2005). A comparison of different print mottle evaluation models has shown that instrumental measurements must consider the amplitude of the variation, the coarseness, i.e. the frequency distribution of the variation in the print, and the mean print reflectance level (Fahlcrantz & Johansson 2004).

3.6.3 Dot gain

Physical dot gain, due to a physical ink spreading, is caused by the pressure between the printing plate and the substrate. Besides physical dot gain, optical dot gain may also arise. While the former is a real enlargement of the dot, the latter is an illusion of ink spreading. When light hits a printed dot it will be diffused and reflected from the surface. Some of the reflected light will pass through the edges of the dot, and the viewer will see a halo around the dot as shown in Figure 29. This halo cannot be separated from the real dot using only the naked eye and it will look like a printed area.

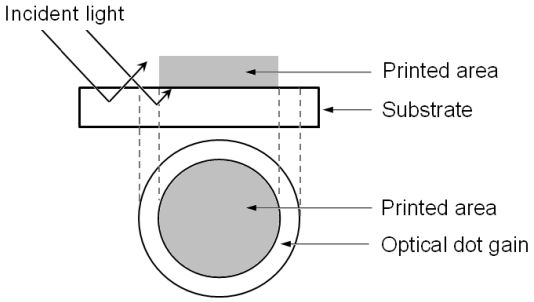

Figure 29. Optical dot gain. Incoming light is scattered in and reflected from the substrate. The light that scatter in the substrate and disappears under the dot will create a shadow.

Although these two dot gain phenomena are of different nature, they are often considered as a single total dot gain, or absolute dot gain. The absolute dot gain can be expressed using the Murray-Davies equation (Murray 1936):

$$Dot\ gain = \left[\frac{(1-10^{-D_R})}{(1-10^{-D_V})}\right]\cdot 100 - F_{nom} = F_D - F_{nom} \qquad [10]$$

where D_R is the half tone density, D_V is the solid tone density, F_{nom} is the nominal tone value of the printing plate and F_D is the effective coverage of the print.

3.6.4 Print gloss

The print gloss is related to the amount of light that is reflected from the printed surface at the same but opposite angle to the normal of the incident light. The specularly reflected light is not affected by the printed surface and leaves the surface with unchanged spectral composition. This means that if a dark printed area is illuminated with white light, the specularly reflected light from that surface will be just as white as the incident light. As discussed in section 3.5.1, gloss is strongly related to the ink setting process. In addition, gloss is also related to the surface roughness. The smoother the surface, the higher is the measured gloss (Figure 10). A low print gloss is an indication of a rough print surface, and this often means that the print density is also low, resulting in a poor image and poor colour reproduction (Oittinen and Saarelma 1998). The print gloss and the gloss contrast are thus important factors when a high quality print is desired.

The gloss contrast, i.e. the difference between the paper gloss and the print gloss, also called "snap", is important for the readability of a printed text or the appearance of a printed image. The gloss contrast can be expressed as (Oittinen and Saarelma 1998):

$$\Delta G = G_{pr} - G_{pa} \qquad [11]$$

where ΔG is the gloss contrast, G_{pr} is the print gloss and G_{pa} is the paper gloss.

The printed areas should have a higher gloss than the base paper, a positive snap, to make the image appealing (Preston et al. 2002). As shown in Figure 30, the resulting print gloss is strongly affected by the surface roughness of the substrate. If the roughness depth of the paper is less than the thickness of the ink layer (left-hand image in Figure 30), the ink can fill the rough profile of the paper and the gloss contrast will be high. On the other hand, if the paper is too rough (right image in Figure 30), the gloss contrast will be low. A consequence of this is that a highly glossy substrate results in a very glossy print, but if the gloss value of the substrate is too high, the gloss contrast may decrease or even become negative (Preston et al. 2002).

Figure 30. The gloss contrast, or the difference between paper gloss and print gloss. A fairly rough paper, as in the left image, gives a smooth and glossy print. The right image however, shows a very rough substrate that results in a low print gloss.

Other studies have confirmed the smaller difference in paper and print gloss in offset printing (Rousu et al. 2005). The authors showed that high coating gloss leads to high print gloss. The snap increased with increasing sheet gloss to a value of 33-35 %. After that, the snap decreased, which was attributed to the surface structure of the coated paper. The ink smoothed out the surface and thereby created a higher gloss, but only up to a critical point.

Due to the impact of the paper surface roughness on the print gloss, the coating colour recipe and the resulting coating layer properties are of utmost importance for the print quality. A higher surface porosity often results in a faster ink setting which leads to a greater ink penetration in the z-direction, a lower print gloss and a lower print density (Preston et al. 2008; Preston et al. 2002). However, the ink recipe also affects the ink setting. Rheological measurements of water-based flexographic inks have shown that the interaction between water and the components of the ink determines the water retention. A low dewatering rate resulted in a higher print gloss due to the prolonged leveling time (Olsson et al. 2007).

4 Modeling of optical properties

4.1 The Kubelka-Munk theory

The Kubelka-Munk (KM) theory was originally developed for paint films (Kubelka & Munk 1931)but it has for a long time been used for modelling the optical properties of paper and paper coatings. Limiting assumptions are a flat surface, that both absorbing and scattering substances must be distributed evenly through the layer, and that any particles present must be much smaller than the total thickness of the coating layer. The theory works best when the illumination source is diffuse monochromatic light and the light absorption of the material is low. An ideal situation is when more than 50 % of the light is reflected and less than 20 % is transmitted. The KM model (Figure 31) is not therefore suitable for dyed or very dark materials (Yang 2002).

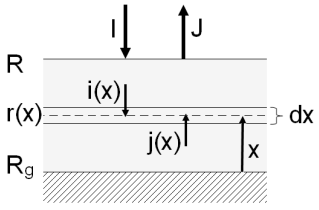

Figure 31. Parameters used in the Kubelka-Munk model.

The KM model as used in the paper industries measures the reflected light in relation to that reflected under the same conditions from the perfect reflecting diffuser to calculate the reflectance factor, R. R is measured against a black background, R_0, and against an opaque pad of papers, R_∞. In cases where the quantity of material is limited, R_∞ can be calculated using equations [2] and [3] presented in section 2.6.2.

The reflectance factor values can then be used to calculate the light scattering coefficient, *s*, and the light absorption coefficient, *k*, according to the following equations:

$$s = \frac{1}{w \cdot \left[\frac{1}{R_\infty} - R_\infty\right]} \ln\left[\frac{(1 - R_0 R_\infty) R_\infty}{(R_\infty - R_0)}\right] \qquad [12]$$

$$k = \frac{s \cdot (1 - R_\infty)^2}{2 \cdot R_\infty} \qquad [13]$$

where w is the grammage of the sample (kg/m^2). The properties of a two-layered structure AB placed over either a black background or over an infinitely thick pad can be calculated:

$$R_{0,AB} = R_{0,A} + \frac{T^2{}_A \cdot R_{0,B}}{\left(1 - R_{0,A} \cdot R_{0,B}\right)} \qquad [14]$$

$$R_{\infty,AB} = \frac{1 + R_{0,AB} \cdot R_{0,BA} - T^2{}_{AB}}{2 \cdot R_{0,BA}} - \sqrt{\left(\frac{1 + R_{0,AB} \cdot R_{0,BA} - T^2{}_{AB}}{2 \cdot R_{0,BA}}\right) - \frac{R_{0,AB}}{R_{0,BA}}} \qquad [15]$$

where A and B represent the two different layers and T is the transmittance of layer A, or the combination of both layers. The transmittance is calculated using equation [16] (Pauler 1999).

$$T = \sqrt{\left(\frac{1}{R_\infty} - R_0\right) \cdot \left(R_\infty - R_0\right)} \qquad [16]$$

Experiments have been focused on modelling the influence of non-uniform reflectance induced by the surface structure, and how it affects the diffuse reflectance factors obtained using the standardized d/0° measurement geometry (Granberg et al. 2003a). The scattering coefficient, *s*, often decreases with increasing coat weight when the KM model is used. This has been explained as being due to a change in the structure and porosity of the coating layer, or as an effect of penetration of the coating into the paper. However, a more recent article (Granberg et al. 2003b) explained this as a non-uniform reflectance distribution that influences the KM-fitted data. They used three different substrates, with absorbent and non-absorbent properties, and concluded that the surface reflectance of the substrate and of the coated substrate can explain the apparent decrease in s as an artefact when a sample is measured with an instrument having a d/0° geometry.

The behaviour and interpretation of the light absorption and light scattering coefficients, k and s respectively, for the KM model has been investigated (Granberg & Edström 2003). Recent studies have shown that both the k value and

the k/s ratio increase non-linearly with increasing dye concentration. This has been explained by an intrinsic error in the KM model induced by light absorption that tends to orient the light fluxes perpendicular to the plane of the sheet.

4.2 The radiative transfer theory

The KM model is widely used in the pulp and paper industry to predict the brightness and opacity of papers consisting of different pulps, fillers, and coating. The simplicity of the equations is the main reason for their extensive use, and before the introduction of personal computers their simplicity was of even greater advantage. A method usually referred to as "radiative transfer theory" (RT) is a much more complex way of describing and calculating light scattering in paper and print than the simple KM model. RT solves the radiative transfer equations (Thomas & Stamners 2002) and is a general model that divides the light fluxes into a number of channels (Figure 32). The number of channels can be adjusted to fit a specific calculation, but 20 channels are sufficient in normal cases. Several layers having different optical properties can be placed upon each other during a simulation.

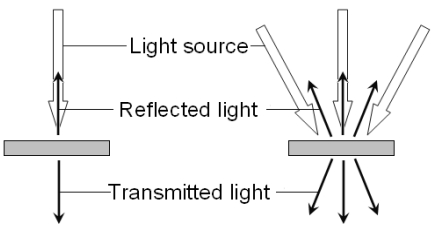

Figure 32. Illustrations of the 2-channel KM model (left) and a multi channel model such as DORT (right).

The KM model uses incoming and reflected light at a specific wavelength, for a given thickness or coat weight, to calculate light scattering, *s*, and light absorption, *k*. RT models on the other hand use light absorption, σ_a, and light scattering, σ_s, coefficients that are physical quantities.

In a RT model, the intensity of the radiation, I, and the loss of radiation due to scattering and absorption, *dI*, in thickness *ds*, are used to define the extinction coefficient, σ_e.

$$\sigma_e = -\frac{dI}{Ids} \qquad [17]$$

The extinction coefficient can then be separated into the light absorption and light scattering coefficients.

$$\sigma_e = \sigma_a + \sigma_s \qquad [18]$$

To be able to consider the direction of scattering, an asymmetry parameter *g* is introduced. The asymmetry parameter has a value between -1 and 1, where 0 represents uniform scattering and other values represents peaked scattering in the forward or backward directions. The light scattering coefficient and the asymmetry parameter are sometimes combined to a reduced scattering coefficient, σ_s', in order to increase the calculation speed.

$$\sigma_s' = \sigma_s \cdot (1 - g) \qquad [19]$$

Expressions that approximately describe the relation between the KM scattering and absorption coefficients, s and k, and the reduced scattering coefficient, σ_s', and the absorption coefficient, σ_a, can be written (Mudgett & Richards 1971) as:

$$s = \frac{3}{4}\sigma_s' - \frac{1}{4}\sigma_a \qquad [20]$$

$$k = 2\sigma_a \qquad [21]$$

A specific RT implementation called DORT2002 (discrete ordinate radiative transfer) has been developed to calculate the optical response given almost any illumination and detection geometry (Edström 2005), and it also handles heavily dyed papers, full-tone prints, gloss and the effects of optical brightening agents (OBA). The KM model is a simple special case of DORT2002, when the light is perfectly diffuse, the scattering is perfectly isotropic and only two channels are used (Figure 32). Under these circumstances the scattering and absorption coefficients for the two models are the same.

When the DORT2002 model was used, and scattering and absorption coefficients calculated from equations [12] and [13] were compared with those calculated from equations [20] and [21], errors of up to 20 % were found in the reflectance factor calculations of the KM model (Edström 2004). In fact, Edström noted that the KM model may fail to provide correct results even under ideal conditions. This means that the previous knowledge gained from using the KM model can be used as a foundation for future work with the DORT2002 model. Both the number of channels and the number of layers of material can be adjusted to fit a specific

calculation. However, as with the KM model, the DORT2002 model assumes a flat surface and cannot be used for simulations of surface roughness.

4.3 Monte Carlo simulations

Instead of solving the radiative transfer equations numerically as the DORT2002 model does, a Monte Carlo method can be used to approach the calculations. Monte Carlo methods use repeated random sampling to compute results and are often used for simulations of physical and mathematical systems over a wide range from gambling and finance to chemical and aerodynamic systems. The method has also been used to describe light behaviour in different materials, such as paper products (Wang et al. 1995).

Open PaperOpt is a Monte Carlo simulation program that has been designed for the calculation of light scattering and light absorption in paper and paper coatings. Using this program, the layer structure of a substrate such as a paper or a coated paper can be described as a geometrical distribution or as a fibre network. This results in a three-dimensional model of the inner paper structure and, unlike the DORT2002 model, Open PaperOpt can also simulate the surface roughness (Coppel & Edström 2009). When a structure has been created, the components within the simulated layer are modelled to interact with the light. Three parameters control the process: σ_a, σ_s and *g*. The probability, *P*, for a light particle to travel a certain distance, t, before a scattering or absorption event occurs is then given by:

$$P(t) = (\sigma_s + \sigma_a)e^{-(\sigma_s+\sigma_a)t} \qquad [22]$$

As with the DORT2002 model, g can be used to set a new direction for the wave packet or, if g is equal to zero, to create a uniform scattering. Surface scattering is treated as a combination of two effects. The long-range topographic structure, called the surface waviness, is the part that deflects incident wave packets according to Snell's law and the Fresnel equations. In addition, the short-range topographic structure, the micro-roughness, scatters the light diffusely. The scattering by the micro-roughness is introduced by allowing a fraction of the reflected and refracted light to be distributed in a Lambertian manner. Within a layer, the scattering process is controlled by the scattering and absorption coefficients.

The average light behaviour is calculated by following the path of a large number of light particles, or wave packets, through the model, as indicated in Figure 33. The light can be absorbed (1), transmitted (2), reflected away from the system (3) or reach the registration point, or the "detector", that can be placed at any location or angle with respect to the surface that is subject to the simulation (4). The large number of wave packets needed for a simulation makes the Open PaperOpt model very time-consuming compared to DORT2002 or the KM model.

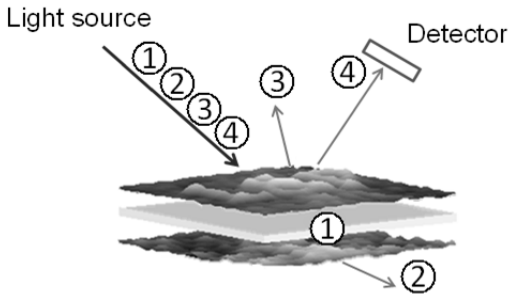

Figure 33. The Open PaperOpt simulation model. One or several layers are considered and equipped with roughness and optical properties. The paths of a large number of light particles are followed, and their average behaviour can be calculated.

5 Materials and methods

5.1 Laboratory scale coating

5.1.1 Objective

The purpose of Paper I was to simulate the decrease in brightness after calendering of coating layers applied on plastic sheets, by using the Open PaperOpt model. By simulating a decrease in surface micro-roughness and an increase in the effective refractive index, the decrease in brightness of the samples could be explained without any change in the coating thickness or any decrease in light scattering. In order to minimise the effect of the substrate and to determine the optical properties of the coating colour alone, a non-absorbent plastic film was used as substrate. In Paper II the investigations were extended to coated paper substrates.

5.1.2 Coating substrate

The non-absorbent plastic film, used in both Paper I and Paper II (Lumirror 54.41, Toray Plastics Europe SA, Miribel, France), had a thickness of 75 μm and a refractive index of 1.6. In Paper II, the substrate was also a four-ply cartonboard, 244 g/m^2, with a bleached top layer, two unbleached centre layers and an unbleached bottom layer (supplied by Korsnäs AB, Sweden).

5.1.3 Coating recipes

A single coating recipe was used for the investigations in Paper I. The coating recipe was 100 parts per hundred parts of pigment (pph) calcium carbonate, a narrow particle size distribution pigment (Covercarb 75, Omya AB, Malmö, Sweden), and 12 pph SB latex with a particle size of 120 nm, and a T_g of 24 °C (Eka Polymer Latex Oy, Oulu, Finland).

For Paper II, four different coating colours were prepared. Two different GCC pigments were used, one with a relatively broad particle size distribution, 90%<2 μm/64%<1μm, and one with a narrow particle size distribution, 95%<2μm/75%<1 μm (Hydrocarb 90 and Covercarb 75, both supplied by Omya AB, Malmö, Sweden), to study the impact of particle packing on the brightness properties. Two styrene-butadiene latices with particle diameters of 120 and 160 nm respectively, both with a T_g of 24 °C (Eka Polymer Latex Oy, Oulu, Finland) were used at 12 pph. The purpose was to investigate the effect of latex particle diameter on the coating structure while keeping all other parameters constant.

As thickener, 0.5 pph carboxymethyl cellulose (Finnfix 10, CP Kelco Oy, Äänekoski, Finland) was used in the recipes for all the coatings prepared in both Paper I and Paper II.

5.1.4 Coating

The coatings were applied by means of a bench coater, K202 Control Coater (RK Print Ltd., Royston, UK) using a series of wire-wound rods. The coatings investigated in Paper I were applied using four different rods, rod 3, 4, 6 and 8. This resulted in coat weights of 16, 26, 43 and 71 g/m^2. Three rods, rod 3, 4 and 6 were used in Paper II, resulting in coat weights of approximately 18, 33 and 48 g/m^2. The coated substrates were dried at 105°C for two minutes in a laboratory oven to ensure good film formation of the latex.

5.1.5 Calendering

A soft-nip laboratory calender (Oy Gradek AB, Kauniainen, Finland) was used, fitted with a heated steel roll and a soft polymer roll. The samples used in Paper I were subjected to 1-10, 15 and 20 nips at a line load of 300 kN/m. Before calendering, and after each of the first ten nips and after the fifteenth and the twentieth nip, the gloss and brightness were measured. For Paper II, the samples were exposed to two calendering conditions: one nip at 100 kN/m and three nips at 100 kN/m. Both uncalendered and calendered samples were investigated. All the trials were performed at a calender speed of 34 m/min, and a calendering temperature of 50°C in a controlled climate room of 23°C and 50 % RH.

5.1.6 Measurement of optical and structural properties

Gloss measurements were made using a gloss meter (Zehntner glossmeter, 20°-75°, Shropshire, UK) at 75° according to ISO 8254-1. For the brightness (R_{457}) measurements, a Minolta 3630 Brightness tester (Basildon Essex, UK) was used. The reflectance factors were measured using a black background (R_0), a plastic plate that is a part of the equipment, and a white background (R_∞) consisting of a pile of coated samples. A STFI Thickness tester (M201, Innventia, Stockholm, Sweden) was used for the thickness measurements. Reflectometry (Surftopic imaging reflectometer, Surfoptic Ltd, Hereford, UK) was used to measure the refractive index and the micro-roughness. All of these measurements were carried out at 23°C and 50 % RH.

5.1.7 Modeling of optical properties

In Paper I and Paper II, Open PaperOpt (Coppel & Edström 2009) was used to model the optical properties of the coating layers and to compute their spectral

reflectance factors in a d/0° geometry. The model allows the surface roughness and the refractive indices of the coating layer and the plastic film to be taken into account. The effect of calendering on the measured optical properties of the coating layer could then be studied separately in terms of changes in surface roughness, internal structure and refractive index at the coating surface. In the simulations, results from measurements of micro-roughness and effective refractive index were used, and the light scattering was optimized to reach the measured brightness decrease of the physical samples.

5.2 Pilot coating

The aim of Paper III was to print pilot-scale-coated cartonboard and to study the effect of ink penetration on the print quality. The substrate was a three-ply cartonboard with a basis weight of 179 g/m^2 with a core of unbleached pulp sandwiched between a bleached top layer and an unbleached bottom layer (supplied by Korsnäs AB, Frövi, Sweden). The top layer was pre-coated at a coat weight of 11 g/m^2. Top coating was carried out with three different coating colours containing 100 parts of ground calcium carbonate (GCC) of various particle size distribution (PSD), all supplied by Omya AB, Malmö, Sweden: broad PSD (Hydrocarb 90, denoted Broad PSD - 64), narrow PSD (Covercarb 75, denoted Narrow PSD - 75) and broad PSD with small particle size (Setacarb HG, denoted Broad PSD - 90). The figure in the sample denotations refer to the percentage of particles below 1 μm in size (Table 1).

Table 1. Particle size data (supplier information).

Pigment	Specific surface area (m^2/g)	Particles < 2 μm (%)	Particles < 1 μm (%)	Particles < 0.2 μm (%)	Name
Broad PSD	12.5	90	64	17	Broad PSD - 64
Narrow PSD	10.0	95	75	12	Narrow PSD - 75
Small particles, broad PSD	19.2	98	90	30	Broad PSD - 90

The binder was a SB-latex with a Tg of 24°C and a particle size of 120 nm (supplied by Eka Polymer Latex Oy, Oulu, Finland), added at 12 parts per hundred parts of pigment. Sterocoll FD (BASF Paper Chemicals, Ludwigshafen, Germany) was added as thickener at 0.3 parts per hundred parts of pigment. The coating colours were diluted to a target Brookfield viscosity of 1000 mPas (spindle no. 4, 100 rpm), resulting in solids content values of 67% for Broad PSD – 64 and Broad PSD - 90, and 63% for Narrow PSD - 75.

The coating was performed on the pilot machine at Korsnäs AB, Frövi, Sweden at a speed of 500 m/min using a bent ceramic blade held at a blade angle of 19°. The

coated cartonboard was dried by means of four separate IR dryers operated at a power of 20% each, followed by a hot air dryer at a temperature of 160°C. The resulting coat weight was 12 g/m² f or all three top coatings. Calendering was done on-line in a soft nip with a rubber roll of hardness 65°Shore D and a steel roll held at a temperature of 100°C. The line load was set to 100 kN/m.

5.3 Printing

The printing was carried out in an IGT-F1 laboratory flexographic printer (IGT Testing Systems, Amsterdam, NL) at a constant machine speed of 0.3 m/s using an anilox roll with a volume of 3.2 ml/m² and a screen ruling of 180 lines/cm. Printing was done with an anilox force of 30 N and application was done at a printing force of 50 N. A printing plate with a hardness of 70° Shore A and a thickness of 1.7 mm (supplied by Miller Graphics, Sunne, Sweden) was used to print both full-tone areas and half-tone areas of 40 and 60 % tone values. A water-based cyan ink, supplied by Sun Chemical Inks A/S, Skovlund, Denmark, was used. The ink was diluted with de-ionized water to a viscosity of 23 s, as measured with a Zahn cup no 2. Printing, and evaluation of print quality, were done in a controlled climate of 23°C and 50 % RH.

The surface roughness in μm of coated surfaces was determined by a Parker Print Surf (PPS) device operated at a clamping pressure of 1.0 MPa (Testing Machines Inc., New York, USA). Gloss measurements of coated and printed surfaces were performed by means of a gloss meter (Zehntner glossmeter, 20°-75°, Shropshire, UK) at 75° according to ISO 8254-1. The brightness (R_{457}) and reflectance factors were recorded by a Minolta 3630 Brightness tester (Basildon Essex, UK). The pore size distribution of coated surfaces was characterized by an Autopore III mercury porosimeter (Micromimetrics Instrument Corporation, Norcross, GA, USA). Pore sizes in the range of 0.02-1 μm were used for average pore volume and pore radius.

Mottling was evaluated by scanning printed full tone areas of size 43.3 by 43.3 mm at a resolution of 600 dpi by an Epson Perfection V750 PRO scanner, followed by data treatment with STFI- Mottling Expert v1.2 software (Innventia AB, Stockholm, Sweden). The result is given as the coefficient of variation (CV, %) over the distance 0.13-0.25 mm. Microscopic images over the same length scale was recorded with an Olympus BX51 System Microscope. The print density and total dot gain were evaluated by a GretagMacbeth densitometer D19C (Regensdorf, Switzerland).

6 Summary of results

6.1 Paper I

The reflectance factor was found to decrease with increasing number of calendering nips (Figure 34). Calendering led to a decrease in the Kubelka-Munk scattering coefficient and an increase in the absorption coefficient of the coated transparent films (Figure 35).

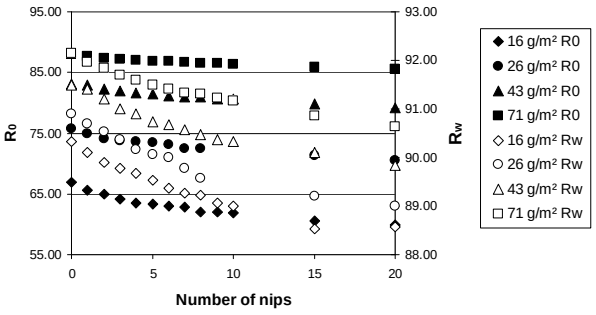

Figure 34. Reflectance factor of coated films over a black background (R_0) and over a white background (R_w). Reflectance factor values decreased with increasing number of nips.

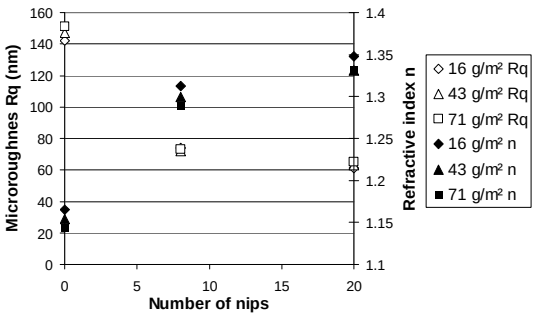

Figure 35. Measured micro-roughness (Rq) and refractive index (n) of the samples with different coat weight plotted versus the number of calendering nips.

Taking into account non-uniform surface reflection at the boundaries between media of different refractive indices, a large part of the reflectance factor decrease due to calendering could be attributed to an increase inthe effective refractive index at the coating surface and a decrease in the surface micro-roughness (Figure

36). To illustrate the effects of changing the simulation parameters, Figure 36 also shows the separate effects of simulating an increase in refractive index and a decrease in micro-roughness for the 16 g/m² samples.

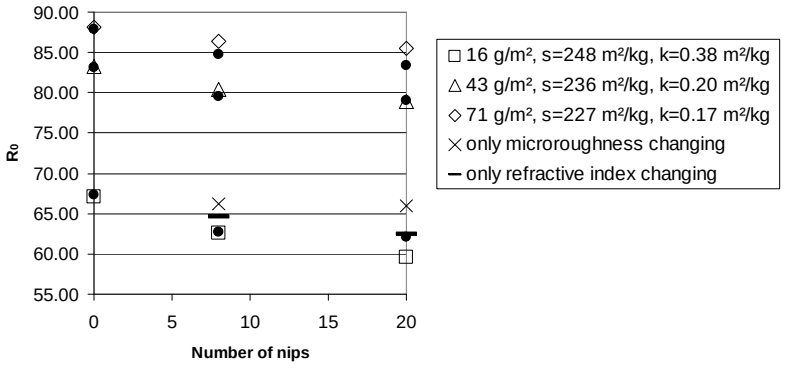

Figure 36. Measured (open symbols) and simulated (dots) reflectance factor of the coated films over a black background. In the simulation, the scattering and absorption coefficients of the coating were kept constant with calendering but the micro-roughness and refractive index were modified according to the measured data.

6.2 Paper II

From simulations based on a two-layer Kubelka-Munk model, it was shown that the brightness decrease of the cartonboard substrate due to calendering makes a negligible contribution to the total brightness decrease of the coated cartonboard. The brightness decrease of the coated cartonboard (Figure 37) was similar to that of the coated plastic film. Using the Kubelka-Munk equations, the light scattering decreased and the light absorption increased (Figure 38). The thickness of GCC-coated plastic films was not affected by calendering, regardless of the pigment and latex size distributions.

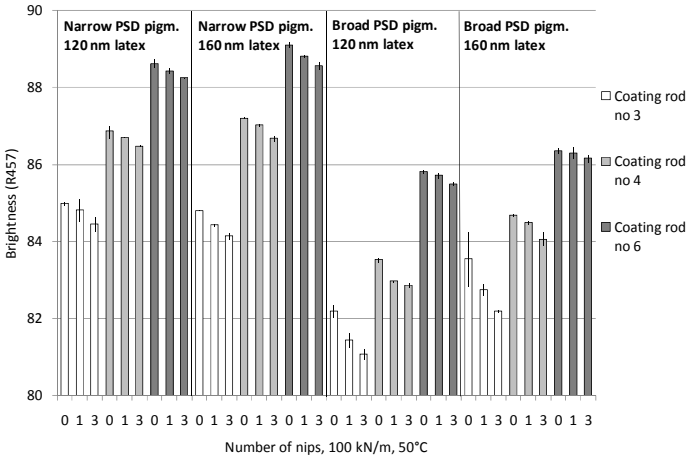

Figure 37. Brightness of the coated cartonboard. The brightness decreased with increasing number of calendering nips. No major change in brightness could be detected in calendered uncoated samples.

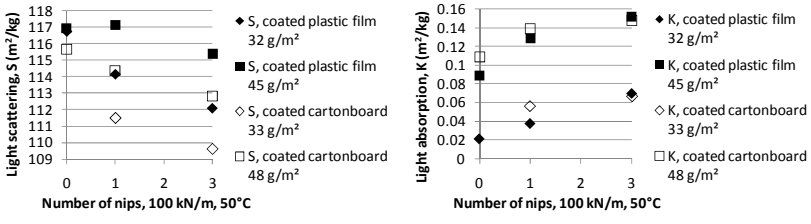

Figure 38. Calculated Kubelka-Munk light scattering (left) and absorption (right) coefficients from both cartonboard and plastic film coated with a narrow particle size distribution and 120 nm latex particle size. S decreased and K increased with increasing number of nips. Both increased with increasing coat weight.

Monte Carlo light scattering simulations (Figure 39), taking into account the measured decrease in the surface micro-roughness and the increase in the effective refractive index showed that surface modifications accounted for most of the observed brightness decrease of the GCC coated substrate, whereas the bulk scattering and absorption coefficients were not affected by calendering. It was also shown that the scattering coefficient was significantly dependent on the coat weight whereas the physical absorption coefficient was not.

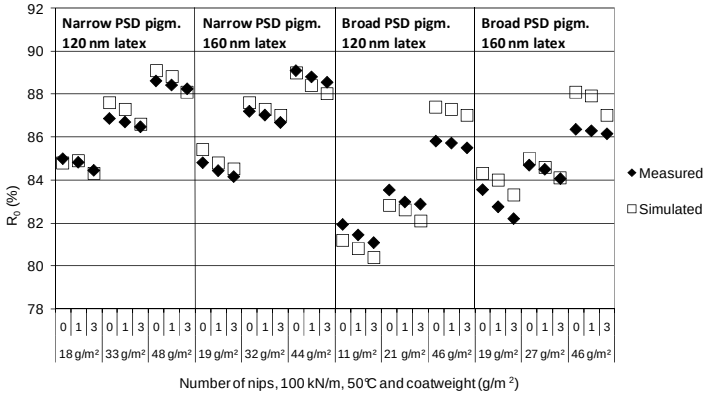

Figure 39. Measured (filled symbols) and simulated (open symbols) reflectance factor for coated cartonboard. The scattering and light absorption coefficients were determined from coated transparent films. Neglecting any modification of the cartonboard substrate, the brightness decrease of these GCC coatings due to calendering can be fully predicted by an increase in the effective refractive index and a decrease in the micro-roughness.

6.3 Paper III

In Figure 40, the pore size distribution and the pore volumes are displayed. The results show a displacement of the curves towards smaller pore diameters after calendering for Broad PSD – 64 and Broad PSD – 90. A change in the pore structure has thus occurred in these samples. The increased pore volume for Broad PSD – 90 after calendering is however unexpected. A possible explanation could be the occurrence of cracks after calendering. Narrow PSD – 75 however show a relatively small change after calendering. A slight decrease in volume can be noticed, but otherwise the shape of the curve for the calendered sample is quite similar to the uncalendered one.

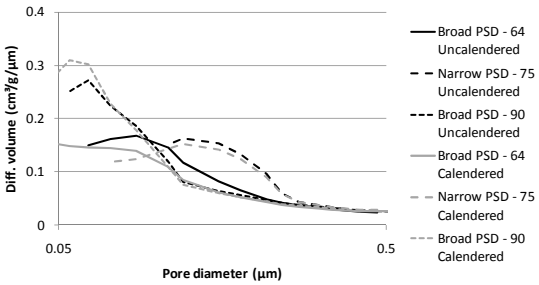

Figure 40. Pore size distribution of uncalendered and calendered samples. Samples Broad PSD – 64 and Narrow PSD – 75 shows a slight decrease in pore volume after calendering while the pore volume of Broad PSD – 90 increases.

The print density, viewed in Figure 41, is clearly lower for Broad PSD – 64 than for the other samples. The difference was confirmed by results from measurements of other prints not presented in Paper III.

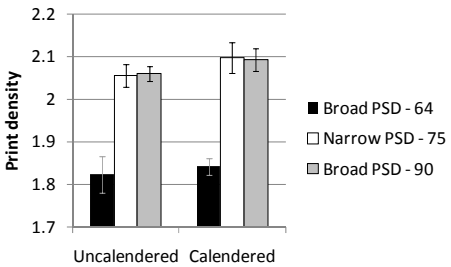

Figure 41. Print density for calendered and uncalendered samples. Broad PSD - 64 clearly has lower values than the other samples.

Figure 42 shows the total dot gain for both 40 and 60 % tone value regions. The low dot gain values for the Narrow PSD – 75 sample indicates that a large pore diameter is important in the printing nip where the ink is mechanically pressed into the pores. No specific trend can however be seen for the resulting dot gain before and after calendering.

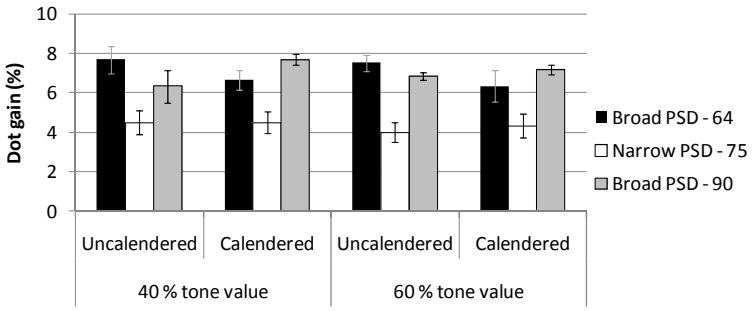

Figure 42. Total dot gain for both 40 and 60 % tone value.

The thicknesses of print layers and mixed layers of ink and coating material were evaluated manually from microscopic images of cross-sections (Table 2). The thickness of the printing layer decreased with calendering for all the samples. However, the thicker ink layer on the uncalendered samples was much more fragmented and uneven than the ink layers on the calendered samples. The thickest ink layer, both for high and low thickness areas, could be found on sample Narrow PSD – 75. Compared to the other samples, the mixed layer was about twice as thick for Narrow PSD – 75.

Table 2. Results from the evaluation of cross-section images given as average values from eight measurements with standard deviation within parentheses.

Sample		Highest thickness values (µm)	Lowest thickness values (µm)	Average thickness (µm)	Thickness of mixed layer (µm)
Broad PSD - 64	Uncalendered	2.29 (± 0.26)	1.35 (± 0.19)	1.82 (± 0.39)	0.51 (± 0.03)
	Calendered	1.95 (± 0.13)	1.08 (± 0.19)	1.52 (± 0.28)	0.40 (± 0.08)
Narrow PSD - 75	Uncalendered	3.11 (± 0.17)	2.23 (± 0.07)	2.67 (± 0.26)	1.08 (± 0.01)
	Calendered	2.90 (± 0.13)	1.15 (± 0.07)	2.03 (± 0.48)	0.91 (± 0.10)
Broad PSD - 90	Uncalendered	2.77 (± 0.17)	1.69 (± 0.23)	2.23 (± 0.34)	0.54 (± 0.11)
	Calendered	2.50 (± 0.06)	1.49 (± 0.08)	1.99 (± 0.28)	0.54 (± 0.01)

The print quality is likely to be dependent on a combination of differences in ink transfer and ink setting on the substrates. Print density increased and dot gain decreased as the coating pore structure became more open.

7 Conclusions

Calendering of coated plastic film lead to a decrease of the Kubelka-Munk scattering coefficient and an increase of the absorption coefficient. This could have been attributed to a change of the coating structure and porosity, which was however not supported by the fact that the thickness remained constant after calendering. Taking into account non-uniform surface reflection at the boundaries between media of different refractive indices, the decrease of the reflectance factors could instead be attributed to a change of the refractive index and micro-roughness at the coating surface. Even though results from previous studies have shown a compression of coating layers containing pure GCC pigments after calendering, the results presented in this theses, using GCC pigments of a broad PSD, showed no such thickness decrease.

When exposed to the same calendering conditions, the brightness decrease for both the coated transparent films and the coated cartonboard was of similar magnitude. The substrate thus had a negligible influence and the observed brightness decrease should therefore be attributed to changes in the coating layer. Given that the thickness of the coated non-deformable plastic films remained constant, it is reasonable to believe that the bulk scattering was not affected in the calendering conditions used in this study. Most of the brightness decrease was instead attributed to a modification of the coating surface micro-roughness and effective refractive index. The decrease of micro-roughness leads to more specular reflection that does not reach the detector. A larger impact was found from the change in effective refractive index. Densification at the top surface leads to an increase of the effective refractive index and an increase of the internal reflection not fully compensated by an increase of the first surface reflection.

The surface of a close- packed coating layer containing a pigment of broad PSD was affected by calendering. The gloss value increased, but both the porosity results and the decrease of light scattering indicates that the inner structure of the coating layer is relatively unaffected by the compression. When printed, both coatings with a larger pore size and a larger pore volume showed a higher print density and a lower print mottling at a small length scale than a more close-packed coating layer. The coating layer with large pore size had the lowest dot gain value, which can be attributed to a larger amount of ink pressed into the more open structure.

8 Future work

Future work involves further investigations of pilot-scale-coated material. A variation of coating recipes containing both GCC and kaolin clay in different proportions are going to be studied. Coatings containing variations in latex particle size and latex amount may also differ in optical properties after calendering. The possible locally closed areas that are believed to have a strong affect on the mottling will also be simulated and investigated.

Important properties to consider in future work are surface structures, porosity, ink distribution in the z-direction and subsequent effects on print quality. Modeling and model verification will be involved in all the studies.

9 Acknowledgements

I first wish to thank my main supervisor Associate Professor Caisa Johansson for all her help. Thank you Caisa for always being supporting, for your positive attitude and for always keeping a good atmosphere!

I also thank my assistant supervisors Professor Per Edström and Associate Professor Magnus Lestelius for structuring my work and my thoughts, and Professor Lars Järnström for all our constructive discussions. Thank you all for your support.

Ludovic Gustafsson Coppel is thanked for good collaboration in this project. Thank you Ludovic for your patience and for all your help. I also want to thank the PhD students and all the associated members of the PaperOpt project for their support.

The Swedish Governmental Agency for Innovation Systems (VINNOVA) and the industry participants in the PaperOpt project are gratefully acknowledged for their financial support. Korsnäs Frövi is thanked for performing the pilot coating. Imerys, Eka Polymer Latex, Omya and SCA are thanked for supplying material and for performing measurements. Stora Enso is thanked for providing equipment. Thank you all for taking an interest in my work and for your engagement.

Associate Professor Anthony Bristow is thanked for the linguistic review of this thesis. Thank you for not only correct my language, but also for guidance and help regarding the content. Dr Christophe Barbier is also thanked for his valuable comments on the content of this thesis.

My friends and colleagues at Karlstad University are thanked for all their help and support, and also for reminding me of coffee breaks and lunch times.

Finally I want to thank my family for their understanding and support.

10 References

Al-Turaif, H. A.; Bousfield, D. W. (2005). *The influence of pigment size distribution and morphology on coating binder migration.* Nordic Pulp and Paper Research Journal, 20 (3), 335-344.

Arney, J. S.; Ye, L.; Wible, J.; Oswald, T. (2006). *Analysis of paper gloss.* Journal of Pulp and Paper Science, 32 (1), 19-23.

Aschan, P.J. (1973). *Drying of Coated Board and Binder Migration.* Tappi Journal, 56 (4), 78-81.

Bakker, J. W. P.; Bryntse, G.; Arwin, H. (2004). *Determination of refractive index of printed and unprinted paper using spectroscopic ellipsometry.* In The 3rd International Conference on Spectroscopic Ellipsometry, July 6, 2003 - July 11. Vienna, Austria: Elsevier. 361.

Berns, R. S. (2000). *Billmeyer and Saltzman's Principles of Color Technology.* (3rd ed.). USA: John Wiley & Sons, Inc.

Bohnenkamp, B., Tietz, M.; Trefz, M. (2005). *New development results of curtain coating for various paper grades.* In 2005 TAPPI Coating Conference and Exhibit, April 17, 2005 - April 20. Toronto, ON, Canada: TAPPI Press. 311.

Caner, E.; Farnood, R.; Yan, N. (2008). *Relationship between gloss and surface texture of coated papers.* Tappi Journal, 7 (4), 19-26.

Chinga, G.; Helle, T. (2003). *Relationships Between the Coating Surface Structural Variation and Print Quality.* Journal of Pulp and Paper Science, 29 (6), 179-184.

Chinga, G.; Helle, T.; Forseth, T. (2002). *Quantification of structure details of LWC paper coating layers.* Nordic Pulp and Paper Research Journal, 17 (3), 313-318.

Coppel, L. G.; Edström, P. (2009). *Open Source Monte Carlo Simulation Platform for Particle Level Simulation of Light Scattering from Generated Paper Structures.* Papermaking Research Symposium. Kuopio, Finland: Papermaking Research Symposium.

Dahlström, C.; Uesaka, T. (2009). *New insights into coating uniformity and base sheet structures.* Industrial and Engineering Chemistry Research, 48 (23).

De Grace, J. H.; Mangin, P. J. (1983). *A Mechanistic Approach to Ink Transfer Part I: -Effect of Substrate Properties and Press Conditions.* London, UK: Banks, W.H., Ed. Pentech Press. 312-332.

Dean, T. W. R. (1997). *The Essential Guide to Aqueous Coating of Paper and Board.* Leatherhead, United Kingdom: Paper Industry Technical Association.

Desjumaux, D. M.; Bousfield, D. W.; Aurenty, P. (1998). *Dynamics of ink gloss: Influence of ink rheology on leveling.* In Proceedings of the 1998 Technical Association of the Graphic Arts, TAGA, April 26, 1998 - April 29. Chicago, IL, USA: TAGA. 618.

Dobler, F.; Holl, Y. (1996). *Mechanisms of Particle Deformation During Latex Film Formation.* ACS Symposium Series, (648), 22-22.

Edström, P. (2004). *Comparision of the DORT2002 radiative transfer solution method and the Kubelka-Munk model.* Nordic Pulp and Paper Research Journal., 19 (3), 397-403.

Edström, P. (2005). *A fast and stable solution method for the radiative transfer problem.* SIAM Review, 47 (3), 447-468.

El-Sherbiny, S.; Xiao, H. (2005). *Characteristics of clay and GCC pigment coatings containing synthetic polymeric thickeners.* Appita, 58 (2), 116-121.

Elton, N. J.; Preston, J. S. (2006a). *Polarized light reflectometry for studies of paper coating structure Part II. Application to coating structure, gloss and porosity.* Tappi Journal, 5 (8), 10-16.

Elton, N. J.; Preston, J. S. (2006b). *Polarized light reflectometry for studies of paper coating structure. Part I. Method and instrumentation.* Tappi Journal, 5 (7), 8-16.

Emilsson, P.; Veyre, J. (2009). *INVOreg tip: A new metering element for coating of board and paper.* ATIP.Association Technique de L'Industrie Papetiere, 62 (5), 12-15.

Endres, I.; Engström, G. (2005). *Influence of calendering conditions on paper surface characteristics - A comparison between hard-nip, soft-nip, and extended soft-nip calendering.* Tappi Journal, 4 (9), 9-14.

Fahlcrantz, C.; Johansson, P. (2004). *A comparison of different print mottle evaluation models.* In 56th Annual Technical Conference of the Technical Association of

the Graphic Arts, TAGA 2004, April 20, 2004 - April 20. San Antonio, TX, United states: Technical Association of the Graphic Arts. 511.

Fujiwara, H.; Fujisaki, N.; Shimizu, I.; Kano, I. (1989). *Effect of water penetration on offset mottling.* Tappi Journal, 72 (5), 91-97.

Gane, P. A. C.; Ridgway, C. J. (2009). *Interactions between flexographic ink and porous coating structures.* In *TAPP*I 2nd Annual PaperCon'09 Conference - Solutions for a Changing World, May 31 - June 3. St. Louis, MO, United states: TAPPI Press.

Gane, P. A. C. (2001). *Mineral pigments for paper: Structure, function and development potential (Part II).* Wochenblatt fuer Papierfabrikation, 129 (4), 176-179.

Granberg, H.; Edström, P. (2003). *Quantification of the intrinsic error of the Kubelka-Munk model caused by strong light absorption.* Journal of Pulp and Paper Science, 29 (11), 386-390.

Granberg, H.; Rundlöf, M.; Mattson, L. (2003a). *Influence of the surface-induced nonuniform reflectance on the diffuse reflectance factor. Part I: model predictions.* Journal of Pulp and Paper Science, 29 (8), 247-253.

Granberg, H.; Rundlöf, M.; Mattson, L. (2003b). *Influence of the surface-induced nonuniform reflectance on the diffuse reflectance factor. Part II: experimental verification on coated substrates.* Journal of Pulp and Paper Science, 29 (8), 254-259.

Holmvall, M.; Lindström, S. B.; Uesaka, T. (2010). *Simulation of two-phaseflow with moving immersed boundaries.* International Journal for Numerical Methods in Fluids, Published online in Wiley Online Library, DOI: 10.1002/fld.2484.

Johnson, J.; Ratto, P.; Lestelius, M.; Harnström, L. (2003). *Dynamic nip pressure in a flexographic CI-printing press.* In TAGA Proceedings 2003: 55th annual conference, Montreal, QC, Canada.

Karipidis, C. (1994). *Bestämning av ett arks (skikts) optiska egenskaper med tvåbakgrundsmetoden (Licentiate Thesis).* Diss. Kungl. Tekniska Högskolan, Stockholm, Sweden: Institutionen för Pappers och Massateknik.

Kenttä, E.; Pohler, T. (2008). *How latex distribution is affected by changes in coating structure -Results from a pilot study.* In *TAPP*I Advanced Coating Fundamentals Symposium, June 11-13. Montreal, QC, Canada: TAPPI Press. 22.

Kipphan, H. (2001). *Handbook of Print Media, Technologies and Production Methods.* (1st ed.). Berlin, Germany: Springer.

Koivula, H.; Preston, J. S.; Heard, P. J.; Toivakka, M. (2008). *Visualisation of the distribution of offset ink components printed onto coated paper.* Colloids Surf., 317 (1-3), 557-567.

Kramm, A.; Mair, B. (2010). *Coating technology of yesterday and tomorrow in paper manufacture in the same house; Streichtechnik gestern und morgen in einem Haus.* Wochenblatt fuer Papierfabrikation, 138 (6), 496-497.

Kubelka, P.; Munk, F. (1931). *Ein beitrag zur optic der farbanstriche.* In Ein beitrag zur optic der farbanstriche. *Z.* Tech. Phys. 593-601.

Kuehni, R. G. (1997). *Color, an Introduction to Practice and Principles.* USA: John Wiley & Sons, Inc.

Kugge, C. (2004). *An AFM study of local film formation of latex in paper coatings.* Journal of Pulp and Paper Science, 30 (4), 105-111.

Lamminmaki, T.; Forsstrom, U.; Tienari, M.; Saharinen, E.; Mikkila, J.; Koskelainen, J. (2005). *Calendering of coated paper at high speeds and temperatures.* Nordic Pulp and Paper Research Journal, 20 (3), 354-360.

Larson, R. G. (1999). *The Structure and Rheology of Complex Fluids.* New York, USA: Oxford University press.

Larsson, M.; Engström, G.; Vidal, D.; Zou, X. (2006). *Compression of coating structures during calendering.* In 2006 TAPPI Advanced Coating Fundamentals Symposium, Turku, Finland, February 8-10, Session 6. 19.

Larsson, M.; Engström, G.; Vidal, D.; Zou, X. (2007). *Impact of calendering on coating structures.* Nordic Pulp and Paper Research Journal, 22 (2), 267-274.

Lepoutre, P.; De Grace, J. H. (1978). *Ink Transfer Characteristics and Coating Structure.* Paper Technology and Industry, 19 (9), 301-304.

Lindberg, S.; Fahlcrantz, C. (2005). *Perceptual assessment of simulated print noise with random and periodic structure.* Journal of Visual Communication and Image Representation, 16 (3), 271-87.

MacGregor, M. A.; Johansson, P.; Beland, M. (1994). *Measurement of small-scale gloss variation in printed paper. Topography explains much of the variation for one paper.* In

Proceedings of the International Printing and Graphic Arts Conference, October 17- 20. Halifax, Can: TAPPI Press. 33.

Mudgett, P. S.; Richards, L. W. (1971). *Multiple scattering calculations for technology.* Applied Optics, 10 (7), 1485-1502.

Murray, A. (1936). *Monochrome Reproduction in Photoengraving.* Journal of Franklin Institute, vol 221, 721-744.

Niskanen, I.; Raty, J.; Peiponen, K.; Koivula, H.; Toivakka, M. (2007). *Assessment of the complex refractive index of an optically very dense solid layer: Case study offset magenta ink.* Chemical Physics Letters, 442 (4-6), 515-517.

Niskanen, K. (1998). Paper Physics, in Gullichsen, J.; Paulapuro, H. (eds). *Papermaking science and technology series, Book 16*. Helsinki, Finland: Fapet Oy.

Oittinen, P.; Saarelma, H. (1998). Printing, in Gullichsen, J.; Paulapuro, H. (eds). *Papermaking science and technology series, Book 13*. Helsinki, Finland: Fapet Oy.

Olsson, R.; Yang, L.; Lestelius, M. (2007). *Water retention of flexographic inks and its influence on final print gloss.* Nordic Pulp and Paper Research Journal, 22 (3), 287-292.

Park, S.; Lee, H. L. (2006). *Influence of the calendering conditions on opacity and quantitative evaluation of the z-directional density variation by image analysis.* Nordic Pulp and Paper Research Journal, 21 (2), 211-215.

Pauler, N. (1999). *Paper optics.* AB Lorentzen & Wettre, Kista, Sweden.

Peiponen, K.; Kontturi, V.; Niskanen, I.; Juuti, M.; Raty, J., Koivula, H.; Toivakka, M. (2008). *On estimation of complex refractive index and colour of dry black and cyan offset inks by a multi-function spectrophotometer.* Measurement Science and Technology, 19 (11).

Preston, J.; Hiorns, A.; Parsons, D. J.; Heard, P. (2008). *Design of coating structure for flexographic printing.* Paper Technology, 49 (3), 27-36.

Preston, J. S.; Gate, L. F. (2005). *The influence of colour and surface topography on the measurement of effective refractive index of offset printed coated papers.* Colloids Surf., 252 (2-3), 99-104.

Preston, J. S.; Elton, N. J.; Legrix, A.; Nutbeem, C.; Husband, J. C. (2002). *The role of pore density in the setting of offset printing ink on coated paper.* Tappi Journal, 1 (5), 3-5.

Rentzhog, M.; Fogden, A. (2005). *Influence of formulation and properties of water-based flexographic inks on printing performance for PE-coated board.* Nordic Pulp and Paper Research Journal, 20 (4), 410-417.

Rounsley, R. (1991). *How Paper Properties can be Develpoed Using Different Methods of Calendering.* Tappi Journal, (74 (1)), 105-109.

Rousu, S.; Gane, P.; Eklund, D. (2005). *Print quality and the distribution of offset ink constituents in paper coatings.* Tappi Journal, 4 (7), 9-15.

Rättö, P.; Rigdahl, M. (2001). *The influence of temperature on the compression behaviour of paper in the thickness direction.* Nordic Pulp and Paper Research Journal, 16 (3), 178-182.

Sadovnikov, A.; Lensu, L.; Kalviainen, H. (2008). *On estimation of perceived mottling prior to printing.* In Image Quality and System Performance V. USA: SPIE - The International Society for Optical Engineering.

Ström, G.; Englund, A.; Karathanasis, M. (2003). *Effect of coating structure on print gloss after sheet-fed offset printing.* Nordic Pulp and Paper Research Journal, 18 (1), 108-115.

Thomas, G. E.; Stamners, K. (2002). *Basic State Variables and the Radiative Transfer Equation.* In Dessler, A.J., Houghton, J.T. and Rycroft, M.J. (eds.) Radiative Transfer in the Atmosphere and Ocean. Cambridge, United Kingdom: Cambridge University Press. Chapter 2.

Tollenaar, D.; Ernst, P. A. H. (1962). *Optical Density and Ink Layer Thickness.* InProceedings of International Conference of Printing Research Institute (IARIGAI). 214-234.

Walker, W. C. (1980). *Determination of Ink Transfer Parameters.* American Society of Mechanical Engineers, Heat Transfer Division, (Publication) HTD, , 127-136.

Walker, W. C.; Fetsko, J. M. (1955). *A Concept of Ink Transfer in Printing.* American Ink Maker (December), 38-44, 69-71.

van de Hulst, H.C. (1981). *Light Scattering by Small Particles.* Mineola, N.Y., USA: Dover Publications, Inc.

Wang, L.; Jacques, S. L.; Zheng, L. (1995). *MCML-Monte Carlo modeling of light transport in multi-layered tissues.* Computer methods and programs in biomedicine, 47 (2), 131-46.

Xiang, Y.; Coleman, P.; Bousfield, D. W.; Osgood, A. (2000). *Cause of backtrap mottle: Chemical or physical?* In 2000 TAPPI Coating Conference and Trade Fair, May 1-4, Washington, DC, USA: TAPPI Press. 45.

Yang, L. (2002). *Modelling Ink-Jet Printing Does Kubelka-Munk Theory Apply?* In IS and T's NIP18: International Conference On Digital Printing Technologies, September 29, 2002 - October 4. San Diego, CA, United states: Society for Imaging Science and Technology. 482.

Zang, Y. H.; Liu, Z.; Cao, Z. L.; Mangin, P. (2008). *An extension of lepoutre mechanism for the consolidation of the structure of latex-pigment coatings.* In TAPPI Advanced Coating Fundamentals Symposium, June 11-13, Montreal, QC, Canada: TAPPI Press. 29.

Optics of coated paperboard

Calendering of coated and uncoated paper is widely used to enhance optical properties such as gloss and print quality. The aim of this thesis is to characterize coatings and prints, and to validate models using experimental results from optical measurements of physical samples.

Calendering of coated paper often leads to a brightness decrease. By comparing simulated and measured results, it was shown that modifications of the surface properties account for the brightness decrease with calendering of substrates coated with ground calcium carbonate. Monte Carlo light scattering simulations showed that surface modifications accounted for most of the observed brightness decrease, whereas the bulk light scattering and light absorption coefficients were not affected by calendering.

The pressure in a printing nip and the porosity of the substrate both affect the amount of ink that is pressed into the porous structure of a coating layer during printing. By printing pilot-coated paperboard with different coating porosities and measuring the resulting optical properties of the prints, a basis for simulations of the different layers was created. Results show that ink distribution is strongly affected by the roughness, the pore size and the pore size distribution of the substrate. A coating layer of broad pigment particle size distribution resulted in a relatively low print density, and comparison of dot gain showed that the coating layer of a narrow particle size distribution had a relatively low dot gain. In this work, these results are explained by the differences in ink distributions on and in the coating layers.

Karlstad University Studies
ISSN 1403-8099
ISBN 978-91-7063-333-1